Electrochemically Regenerated Solvent for Direct Air Capture with Co-generation of Hydrogen at Bench-scale

Final Technical Report

Reporting Period:
October 1, 20201 to February 29, 2024

Principal Authors:
Jinwen Wang, Xin Gao, Ayokunle Omosebi, and Kunlei Liu

University of Kentucky, Lexington, KY

Report Issued
April 2024

Work Performed Under Award Number
DE-FE0032125

SUBMITTED BY
University of Kentucky Research Foundation
109 Kinkead Hall, Lexington, KY 40506-0057

PRINCIPAL INVESTIGATOR
Kunlei Liu
(859) 257-0293
kunlei.liu@uky.edu

U.S. DOE NETL PROGRAM MANAGER
Naomi O'Neil
Naomi.Oneil@netl.doe.gov

SUBMITTED TO
U.S. Department of Energy National Energy Technology Laboratory

ACKNOWLEDGEMENT: UK IDEA is grateful to the U.S Department of Energy National Energy Technology Laboratory for the support of this project. UK IDEA is also grateful to Vanderbilt University and Electric Power Research Institute for support and partnership.

The project team is also grateful to the many UK research personnel for assistance with the project, as listed below.

Patrick Adoba
Tingfei Chen
Xin Gao
Pom Kharel
Kunlei Liu
Emmanuel Ohiomoba
Jesse Okorafor
Ayokunle Omosebi
Roger Perrone
Michael Renfro
Lisa Richburg
Steve Summers
Floyd Taylor
Jinwen Wang

ABSTRACT:
The goal of this final project report is to summarize the work conducted on project DE-FE0032125. In accordance with the Statement of Project Objectives (SOPO), the University of Kentucky Institute for Decarbonization and Energy Advancement (UK IDEA) (Recipient) developed an intensified process to capture CO_2 from ambient conditions (415 ppm CO_2). The process combines low-temperature solvent-aided membrane capture with electrochemically-mediated solvent regeneration to simultaneously capture ambient CO_2 while regenerating the solvent. The technology employs only two primary units, a regenerator and an absorber/contactor, while generating high purity hydrogen as a co-product that can be sold, used for energy storage, or cost-saving depolarization of the direct air capture (DAC) system during the grid peak demand, allowing for flexible operation. Since the technology is powered directly by DC electricity, it can seamlessly tie in with power sources like solar cells without the need for AC/DC converters, therefore allowing for a remote operation to further mitigate greenhouse gas generation toward deploying a negative carbon emissions technology that is completely decoupled from the carbon emissions from the power source for the DAC unit.

The completion of the project results in significant progress toward the Department of Energy's (DOE's) goal of advancing lab and bench-scale DAC systems to a sufficient maturity level that can justify their continued scale-up through the verification testing of the electrochemically regenerated solvent system for DAC with co-generation of hydrogen at bench-scale. The technology addressed the complexities of incumbent DAC systems by demonstrating at ambient conditions (1) low gas-side pressure-drop facile CO_2 capture via an intensified membrane absorber with in-situ regenerated hydroxide as capture solvent, (2) multi-functional electrochemical regenerator for hydroxide regeneration, CO_2 concentration and hydrogen production at less than 3 V, and (3) stable DAC performance including >90% capture with air influent at the CFM scale.

The data from this project enables the completion of Techno-Economic Analysis (TEA) and Life Cycle Assessment (LCA). TEA and LCA demonstrate the potential of the proposed electrochemical solvent-based process to be a viable DAC option. The analysis did not identify any obvious concern for the bench-scale operation and no apparent barriers to implementing UK IDEA carbon capture and solvent regeneration system at a larger scale.

Table of Contents

1. EXECUTIVE SUMMARY

1.1 Overview

The major accomplishments coming from this project are:

1. Developed a 2-unit process operation with more than 90% CO_2 capture at gaseous pressure drop less than 0.2 psi in the membrane absorber (MA) while regenerating the capture solvent at less than 2.7 V in the electrochemical regenerator (ER) by using a catalytic electrode and/or desired concentration of capture solvent with internal recirculation. 2.4 V has been achieved.
2. Achieved H^+/K^+ crossover (through a cation-exchange membrane) ratio of less than 15% in the ER by optimizing a flow channel design, thickness of a spacer, and/or a cation-exchange membrane.
3. Demonstrated a continuous and reliable direct air capture (DAC) pilot process at the air flow rate of 10 CFM with more than 90% CO_2 capture efficiency for more than 100 hours through parametric studies, thereby earning the data for next-scale development.
4. The data from this project enabled the completion of techno economic analysis (TEA). The cost of CO_2 captured is estimated under a 3,500 tonnes CO_2 per year (tpy) capture case and a 14× scale-up to a 49,000 tpy capture case with the contribution of the sale price from cogenerated H_2. For the renewable electrical supply scenario at the 1× scale, a hydrogen price of around $10 per kg of H_2 would be needed to achieve price parity with 45Q carbon credits ($185/t), which could be reduced to around $5 per kg of H_2 at the 14× scale by taking advantage of economies of scale on the balance of plant, as well as the CO_2/H_2 purification unit.
5. Lift cycle analysis (LCA) showed that the overall process impact can be either positive or negative depending on the electricity supply scenarios and H_2 gas accounting method. When low-carbon renewable electricity is utilized, a significant carbon abatement up to 1.36 kg CO_2e (CO_2 equivalent) per kg CO_2 captured on the Global Warming Potential (GWP) impact can be achieved.

UK IDEA developed an intensified process to capture CO_2 from ambient conditions (415 ppm CO_2). Using a two-unit operation comprised of a membrane-aided absorption (MA) or sprayer-aided absorption (SA) and electrochemical regenerator (ER), the process couples solvent-based membrane/sprayer -aided capture with electrochemically-mediated solvent regeneration to simultaneously capture ambient CO_2 while regenerating the carbon capture solvent. A key benefit of the technology is its capability for a seamless tie-in with direct current (DC) electricity power sources like solar cells without AC/DC converters for a remote operation to further mitigate greenhouse gas generation toward deploying a negative carbon emissions technology. Concurrently, the technology also generates hydrogen as a coproduct that can be sold to recuperate CO_2 capture cost, or used for energy storage for grid management, or as feedstock for cost-saving depolarization of the DAC system, therefore offering the flexibility for process integration with various existing applications.

The membrane/sprayer -aided air contactor (AC) and ER were parallelly developed in the project. For the MA, nanofiltration (NF) evaluation preceded SA and MA development, for which 140 cm^2 flat-sheet membranes were first down-selected and tested to determine the OH^- separation performance of the membranes, including exploring liquid-side pressure requirements. Experimental testing revealed little to no rejection of OH^- compared to over 70% rejection for carbonates in the feed stream. The required pressure for the operation was estimated at 40 psig, and sweeping CO_2 into the permeate side of the NF membrane assembly decreased the permeate pH commensurate with capture. Next, the NF membrane was scaled-up to a 7.6 m^2 spiral-wound membrane and performance was maintained. A SA was fabricated with BETE spray nozzles and

demonstrated for CO_2 capture from the air with 2 wt% KOH sprayed countercurrent to air influent at 0.3 – 3 CFM. Capture efficiency increased with residence time, achieving 90% capture at gas residence time more than 5 minutes. The capture performance was found to be currently limited by the liquid residence time. By coupling the SA with NF, nearly 100% capture was achieved at about 3 minutes of gas residence, demonstrating process intensification.

For developing the ER, electrode materials including nickel, Inconel (nickel alloy with chromium and iron), platinum, and titanium were first screened in batch mode using a half cell (smaller than 100 mL beaker-style cell, about 0.3 cm^2 electrodes) toward elucidating materials with the best voltametric (voltage-current sweep) response for developing the ER. Inconel was ideal for anode oxygen evolution (and proton production) and sufficient for cathode hydrogen (and hydroxide) production. However, a Pt electrode improved cathode response and current density at similar voltages. Next, a 16 cm^2 flow cell was built, including embedded Inconel serpentine flow fields and current collector, and assembled with Inconel anode and Pt cathode separated by 3 mm. Parametric testing was conducted in constant current mode at 3 A with 0.27-0.95 M K_2CO_3 and 5-15 mL min^{-1}, achieving a performance of 4 V with 0.95 M K_2CO_3 influent at 15 mL min^{-1} to the regenerator. Furthermore, concentration, which partially controls the cell's ohmic resistance, was found to have a stronger impact on voltage minimization. Toward reducing voltage requirement by minimizing charge transport losses, zero anode-cathode gap configuration was explored along with employing the loading factor, a lumped parameter, i.e., current normalized by feed alkalinity and flow rate as a control variable since it affects cell performance, pH swing, and proton crossover. Parametric testing at 1.2-3.06 M K (or Alkalinity), 10-20 mL min^{-1}, and 625 - 1875 A m^{2-} revealed that loading factors below 0.05 achieved less than 20% proton crossover and < 3.75 V, the interim target. A prototype scaled-up ER with approximately 16 × 16 cm^2 active area was fabricated with an Inconel flow field and titanium current collectors. The initial leak testing was completed followed by performance testing and integration with the membrane absorber unit. The system operational limits were evaluated to commission the integrated system. At the end of the project, 2.4 V has been achieved.

The integrated ER and MA were parametrically tested at an air flow rate of 10 CFM and liquid flow rate up to 0.1 gallon min^{-1}, focusing on ER voltage retention at 2.7 V and proton crossover mitigation at 15% and MA capture effectiveness at more than 90%. The ER was further scaled-up with about 21 × 21 cm^2 active area. Long-term operation for up to 100 hours was performed to characterize performance and material degradation, including membranes (ER and MA) and electrodes. After the MA/SA and ER development, integration and performance testing was accomplished, including greater than 100 hours of performance operation to demonstrate initial stability, TEA, and LCA. DAC performance validation on carbon management and energy requirement included in-situ and ex-situ measurements. The in-situ characterization methods included pH, voltage, current, and CO_2 measurements, while ex-situ characterization included inductively coupled plasma spectroscopy (ICP), capture solvent carbon loading, and alkalinity measurements.

1.2 Key Results

This project's successful completion demonstrates that the UK IDEA process, including hydroxide-based CO_2 capture from air coupled with electrochemical solvent regeneration, is an effective, robust, and flexible DAC process. The UK IDEA led team for this project included UK IDEA, EPRI, and Vanderbilt University, with UK IDEA developing the DAC process, Vanderbilt University evaluating the membrane separation, and EPRI performing the TEA and LCA. UK

IDEA's integrated process, including a hybridized nanofiltration membrane/spray tower absorber and ER for CO_2 capture and solvent conditioning, achieved more than 90% capture from air influent at greater than 10 CFM while using smaller than 3.5 V for solvent regeneration. The process generated H_2 as a co-product that can be sold, used for energy storage or cost-saving depolarization of the DAC system during peak demand, and the process achieved a much lower energy requirement. The testing and data collected from the more than10 CFM process provided a clear path for developing a TRL more than 5 process through scale-up and validation at a more than 1,000,000 L hr^{-1} scale process in the future. Summaries of activities from the key tasks are provided below.

Development of an Integrated Membrane Absorber for Effective DAC (Task 2):

UK IDEA in collaboration with project partner Vanderbilt University screened a series of commercial membranes including Synder NFX, Filmtec NF270, and Microdyn Nadir NP030. These membranes achieved 100% OH^- permeance from influent stream with a nominal selectivity ratio of about 4 for OH^-/CO_3^{2-}. The results from membrane testing demonstrated adequate hydroxide separation and satisfied the project's requirement. Several spray nozzles from two vendors (BETE – PJ20, PJ24, PJ32 and Spraying Systems Co. – HP10, HP15, HP20) were evaluated for the spray section of the hybrid membrane absorber (MA) by varying pressure drop, flow rate, and droplet size. Boosting solvent concentration improves capture performance to achieve the more than 90% capture target. During testing with 3M KOH as capture solvent and air influent at 10 cfm (gas residence of 0.7 minutes), the MA achieved 90% capture efficiency.

Development of an Electrochemical Regenerator Cell for Effective DAC (Task 3):

UK IDEA developed an electrochemical flow cell for solvent regeneration at low voltage, with initial material selection performed in beaker-style half-cells (electrodes in one chamber) and H-cells (a membrane separating the two electrodes in the cell). Cyclic voltammetry (scan voltage, while measuring current in forward and reverse direction to return to starting voltage) was performed in the half-cell with Inconel (Ni-Fe-Cr), platinum (Pt), nickel (Ni), iron (Fe), nickel-iron alloy (Ni-Fe), and titanium (Ti) evaluated as the working electrode, and from testing, Inconel was chosen as the electrode for electrochemical flow cell construction due to its suitable anodic and cathodic performance. Ni-Cu/Ni-Cu, Pt-based electrode/Ni-Cu, and Ti/Ti were tested as anodes/cathodes. The electrochemical flow cell was formed with a cation exchange membrane (Nafion or Aquivion), sandwiched by a flow space, which in turn is sandwiched by Inconel/Ti electrodes and endplates with inlet-outlet ports. Parametric studies, including solvent flow rate at 10 - 20 mL min^{-1}, applied current density at 625 - 1875A m^{-2}, and solvent concentration of 1.2 - 3.06 M K^+, confirmed that as the loading factor increased, the (i) pH decreased at the anode but increased at the cathode, (ii) alkalinity decreased at the anode but increased at the cathode, consistent with K^+ transfer from the anode to the cathode via the cation exchange membrane, and (iii) carbon loading remained relatively constant at the cathode but decreased at the anode consistent with the cathode generated hydroxide balancing K^+ transferred. The ER produced near pH 13 -14 solvent for use in the MA for CO_2 capture and achieved a maximum CO_2 to O_2 ratio of 1.6.

Integration of the MA and ER for DAC (Task 4):

UK IDEA integrated an electrochemical regeneration cell with a membrane-spray absorber to scrub CO_2 directly from air and demonstrated their continuous operation. Testing was performed where the carbon rich solvent was conditioned by the ER, followed by recirculating the carbon lean solvent in the MA for CO_2 capture, during which the regenerator remained running. The

integrated unit with the cathode-produced solvent achieved > 90% CO_2 capture from air influent at 10 cfm, approximately 0.7 minutes residence time. The unit attained the target of demonstrating a DAC process with 10 cfm influent air with < 0.2 psig gas-side pressure drop, > 90% CO_2 capture for >100 hours, < 2.7 V of operating voltage, and < 15% of H^+/K^+ crossover ratio through the membrane. In addition, a new 3-channel ER was developed, including a bipolar membrane for in-situ CO_2 purification.

Parametric study and long-term operation (Task 5):

Following process integration and commissioning, the integrated DAC system was parametrically tested by applying different charging currents ranging from 5 to 15 A to the ER. The system's objective was to regenerate the capture solvent used for decarbonizing air, flowing at 10 cfm. In the setup, the influent air was introduced at the bottom of the MA, with the capture solvent sprayed from the top. The system's performance was monitored through voltage, current, pH, and CO_2 sensors, and nitrogen gas was used as a dilution gas for the anode gas exhaust due to instrumentation limitations. During the tests, the integrated system successfully achieved a carbon capture rate of over 90%, specifically 92%, from 10 cfm of air for 100 continuous hours while operating at the voltage below 2.7 V, actual achievement of 2.6 V. Solvent regeneration was accomplished at an operating current of 10 A, and carbon recovery was maintained at a load factor of approximately 1, with a potassium transport efficiency exceeding 85%. The integrated system consistently achieved equivalent carbon capture and recovery rates using a low alkalinity solution with a concentration of approximately 1.4 M as the capture solvent.

Techno-economic Analysis (TEA) (Task 6):

The goal of the TEA was aimed at estimating the capital and operating costs for the UK IDEA DAC process followed by CO_2 separation and H_2 production. The capital cost analysis showed that the total plant cost (TPC) is 16 MM, where the main contributors to the capital cost come from ER and CO_2 purification, accounting for 25% and 24%, respectively. In addition, the air contactor or CO_2 absorber only accounts for 8% of TPC. Furthermore, with the process that captures 86% of CO_2 in air to produce 3,500 tonnes per year of pure CO_2 while co-producing 235 tonnes per year of H_2 gas, the power requirement is 2.32 MWe, in which the ER is the larger power user, accounting for 73% of the total power requirement. By converting the power to monetary currency, the cost of CO_2 capture with CO_2 transportation is $1,112 per tonne of CO_2. With the scale factor of 14, the cost of CO_2 capture can be further reduced to $680 per tonne of CO_2. Please note that the revenue from sale of H_2 gas has not discounted these cost values for CO_2 capture.

Life-cycle Analysis (LCA) (Task 7):

The LCA aims to compare the DAC system's environmental impacts to those of systems producing similar products. Various factors such as the production and storage of hydrogen, compliance with safety standards, and the system's development stage (Technology Readiness Level 3) are addressed. The assessment includes different electricity carbon intensity and hydrogen production scenarios. For instance, under the current U.S. grid mix (546 kg CO_2e/MWh), the net impact of the proposed DAC + H_2 system ranges from an increase of 1.39 kg CO_2 emitted per kg of CO_2 captured and permanently sequestered if no credit for hydrogen generation is taken, to an increase of 0.22 kg CO_2 abated for the case where hydrogen production displaces H_2 produced via electrolysis. Conversely, under renewable energy sources (23 kg CO_2e/MWh), there is an overall net abatement of 0.83 kg CO_2 emitted per kg of CO_2 captured and permanently sequestered if no credit for hydrogen generation is taken, and 0.94 kg CO_2 abated for the case where hydrogen production displaces H_2 produced via electrolysis. Results show varying impacts on global warming potential, influenced by factors such as electricity source and hydrogen accounting

method. The study underscores the need for project-specific analysis due to the variability in impacts across scenarios and highlights the importance of renewable energy in achieving significant carbon abatement.

2. BACKGROUND AND TECHNOLOGY DESCRIPTION

2.1. Project Background and Objective

This project developed and evaluated a novel electro-membrane system for the direct air capture of CO_2 toward mitigating the effects of a sustained increase in the atmospheric concentration of the greenhouse gas and its looming climatic implications. For DAC systems, the low concentration of CO_2 in the air, 415 ppm, presents a significant challenge, requiring large energy input for recovery (thermodynamic minimum of 483 kJ kg^{-1} for DAC versus 158 kJ kg^{-1} for post-combustion capture with 90% CO_2 gas recovery) while processing large volumes of air per fraction of CO_2 recovered leading to high-pressure drop and additional energy requirement. Currently, solvent and sorbent-based approaches are under consideration for DAC. Due to the low concentration of CO_2, strong interactions between CO_2 and a capture solvent are required for effective removal, leading to high regeneration costs. Together, these facets make implementing a cost-effective DAC at scale (> 1,000,000 tonnes per year) challenging. The UK IDEA technology employs a low-temperature coupled electrochemical-membrane capture and regeneration technology that simultaneously captures and up-concentrates ambient CO_2 while regenerating the capture media. Concurrently, the technology also generates H_2 as a byproduct that can be sold, used for energy storage or cost-saving depolarization and deoxygenation of the DAC system. H_2 production provides a commercial appeal, unlike other DAC systems' limitation to CO_2 as the only product without further processing steps.

The UK IDEA DAC process is a solvent-based process where the use of KOH as the capture solvent presents several benefits, including chemical stability, recyclability, fast kinetics for CO_2 capture, and near "zero" ppm dissolved CO_2 to maximize the driving force for CO_2 absorption, and the compatibility for cathodic (negative electrode) electrolytic regeneration at low voltages.

The specific objectives of the project were to accomplish the proposed process, including (1) developing a 2-unit process operation with > 90% CO_2 capture at gaseous pressure drop < 0.2 psi in the MA while regenerating the capture solvent at < 2.7 V in the ER by using a catalytic electrode and/or desired concentration of capture solvent with internal recirculation, (2) achieving H^+/K^+ crossover (through a cation-exchange membrane) ratio of <15% in the ER by optimizing a flow channel design, thickness of a spacer, and/or a cation-exchange membrane, and (3) demonstrating a continuous and reliable DAC pilot process at the air flow rate of 10 CFM with > 90% CO_2 capture efficiency for > 100 hours through parametric studies, thereby earning the data for next-scale development. All project success criteria were satisfied and are shown in **Exhibit 2.1.1**

Exhibit 2.1.1 Success Criteria for DE-FE0032125

Success Criteria	Budget Period	% Complete	Accomplishments
1. Membrane absorber achieves > 60% of OH- separation (permeation) from a carbonate feed stream at a liquid delivery rate > 2 L/hour	BP1	100%	NFX nanofiltration membrane showed near-perfect permeance (no rejection) of OH^- and about 75% rejection for a regenerator-relevant test solution composed of 5wt% K_2CO_3 and 0.3wt% KOH influent at 6 L $hour^{-1}$.
2. Electrochemical regenerator achieves < 3.7 V of operating voltage and < 20% of H+/K+ crossover ratio through the membrane	BP1	100%	Parametric testing of the flow cell at 1.2-3.1 M K^+, 10-20 mL min^{-1}, and 625 - 1875 A m^{2-} achieved < 20% proton crossover and < 3.7 V at loading factors below 0.05.
3. DAC process with 10 cfm air influent achieves: < 0.2 psi gas-side pressure drop; > 90% CO_2 capture for >100 hours; < 2.7 V of operating voltage; < 15% of H+/K+ crossover ratio through membrane	BP2	100%	• DAC system, including integrated membrane absorber and ER, achieved the milestone requirement of > 90% capture (92% achieved) from 280 L/min (10 cfm) air for 100 hours at < 2.7 V (< 2.6 V achieved) with solvent regeneration at 10 A and carbon recovery at LF of ~0.4, and potassium transport efficiency >85%. • The gas pressure drop in the absorber is less than 0.1 psi at 10 cfm air influent. • Proton crossover in the regenerator minimized below 15% (BP2 Target) at intermediate 0.5 and high 0.98 loading factors. • Regenerator stability was demonstrated with voltage maintained at 2.5-2.6 V during the testing of a single cell over a cumulative period of 25+ hours. Stacking reduced voltage to about 2 V.

2.2. Process Description

Unlike capture from point sources, the low concentration of CO_2 in the air presents a significant challenge. For example, compared to coal flue gas with 14 vol% CO_2, air possesses 0.04 vol%, a 600 times reduction in concentration and driving force. As a result, strong interactions are required between the dilute CO_2 and the binding media for capture, leading to costly regeneration cycles. The UK IDEA process employs OH^- mediated facile capture from the air and is a near-closed-loop process on the solvent side which involves using only two major unit operations, including an electrochemical regenerator cell (ER) and membrane-sprayer absorber (MA). Unlike typical solvent-based air capture processes requiring elevated temperatures (thermal-swing) for solvent regeneration, it operates under ambient conditions. CO_2 from air is captured in MA with an alkali-

metal OH^--based solvent, and this solvent is regenerated at the ER's cathode (negatively-biased electrode) with H_2 as co-product, simultaneously with CO_2 up-concentration and release for storage or utilization at the anode (positively-biased electrode). A schematic of the UK IDEA DAC process is shown in **Exhibit 2.2.1**.

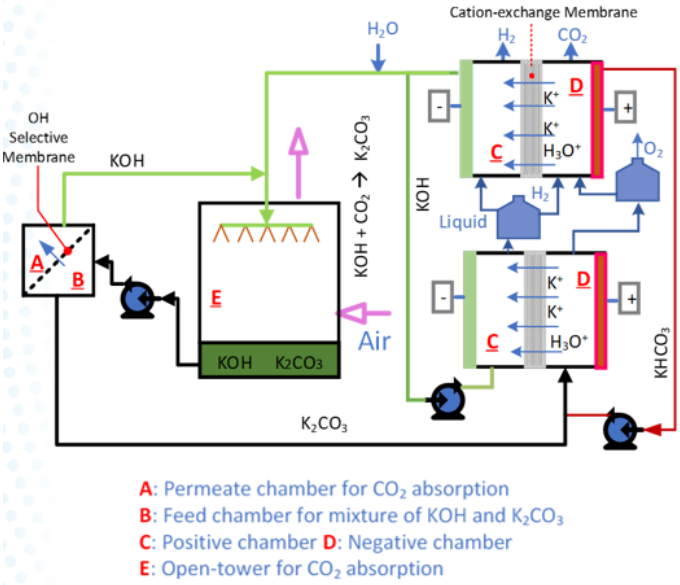

Exhibit 2.2.1. Schematic of UK IDEA MA and ER setup used to capture CO_2 from air and solvent regeneration with the production of H_2.

The MA features nanofiltration membranes with OH-selectivity and a spray tower where influent ambient CO_2 is absorbed into the capture solvent via the membrane and/or the spray tower with the equilibrium CO_2 partial pressure difference between 415 ppm CO_2 in the air (42 Pa) and dissolved CO_2 (0 Pa for KOH), providing the driving force, and reaction with KOH via $CO_{2\,(dissolved)} + 2KOH = K_2CO_3 + H_2O$ providing capture and maintaining the driving force. The rate of CO_2 absorption can be estimated, $R_{CO2} \approx C_{CO2}K_H\sqrt{D_{CO2}kC_{OH}}$ where C_{CO2}, K_H, D_{CO2}, k (~10 $m^3mol^{-1}s^{-1}$), and C_{OH} are the CO_2 concentration in air, Henry's constant, the diffusivity of CO_2, rate constant, and concentration of OH^-, and it follows that reduced and low OH^- concentration resulting from capture leads to diminished capture rate. Counter-current operation is also employed to preserve the driving force. Following capture, $K_2CO_3/KHCO_3$ from the membrane exits to the ER to liberate CO_2 in concentrated form while the OH^- rich solution returns to the spray tower. In the ER, water splitting reactions including the H_2 evolution reaction (HER, $2H_2O$ + electrons = $H_2 + 2OH^-$) and O_2 evolution reaction (OER, $2H_2O = O_2 + 4H^+$ + electrons) control pH.

The $K_2CO_3/KHCO_3$ from MA is fed to the anode side, where K^+ ions in solution are attracted to the negatively charged cathode and are transported via a cation exchange membrane (e.g., Nafion) to the cathode to combine with OH^- (recreating the capture solvent), while CO_3^{2-} or HCO_3^- is converted to CO_2 in sequence by reacting with protons produced at the anode via $CO_3^{2-} + H^+ = HCO_3^-$ followed by $HCO_3^- + H^+ = CO_2 + H_2O$. In the UK IDEA process, the concentration of the K^+-based solvent is adjustable with internal recirculation.

The UK IDEA process operated at room temperature for air contactor and 70 ºC for ER, with initial performance demonstrated in the separate units of the MA and ER before integration. During performance evaluation, pH, flow rate, alkalinity, concentrations, pressure, contact angle, power, voltage, and current were used to assess effectiveness. Details of the process development for the MA and ER are discussed in **Section 3,** along with their results.

3. PROJECT TECHNICAL RESULTS

3.1 Development of an integrated membrane absorber for effective DAC

Nanofiltration aided reclamation of hydroxide capture solvent

In order to design the MA, several commercial NF membranes were considered for procurement, including Synder's polyamide based NFX, NFW, and NDX membranes. The multivalent to monovalent selectivity ratio was employed as a selection criterion. As shown in **Exhibits 3.1.1a** and **b**, their estimated selectivity from monovalent (NaCl) to divalent ($MgSO_4$) rejection ranged from 2 to 60 while achieving adequate water permeance > 0.3 kg $[m^2\text{-hr-psig}]^{-1}$ based on vendor information from Sterlitech.com. From **Exhibit 3.1.1a** and **b**, the NFX membrane was chosen for immediate testing due to its high selectivity and sufficient flux.

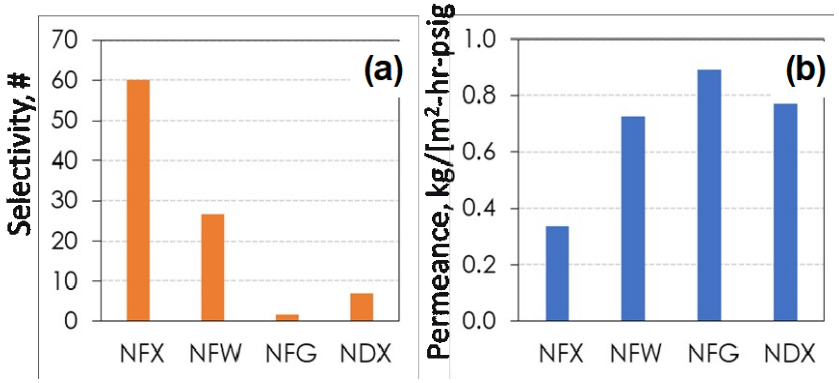

Exhibit 3.1.1. Selectivity (a) and permeance (b) of candidate nanofiltration membranes.

After procuring a flat-sheet Synder NFX membrane, it was tested for hydroxide recovery from a feed solution containing 5 wt% K_2CO_3 and 0.3 wt% KOH, pH 12.33, a process relevant composition from the absorber using the setup shown in **Exhibit. 3.1.2.** The SEPA CF unit (Sterlitech) contained the membrane under test, sandwiched and sealed between two stainless blocks clamped down and sealed using a hydraulic hand pump. The feed solution was circulated at 100 mL/min. If a rejection of 100% is assumed (i.e., no selective permeation), the osmotic pressure estimated from Van't Hoff equation ($P = \sum C_i RT$) for the test solution is 421 psi. The flux performance of the membrane was evaluated at multiple pressures with the test solution, and de-ionized water was tested for comparison. **Exhibit 3.1.3** clearly shows permeation at a pressure less than the osmotic requirement assuming 100% rejection, implying the presence of salt (via permeation) on both sides of the membrane. Extrapolation of the performance data for the CO_3^{2-}-containing feed suggests an osmotic requirement of <75 psig by considering the x-axis intercept of the performance line, which implies a leak-free system can be more easily fabricated when coupled with a large area membrane to minimize the pressure requirement for flow.

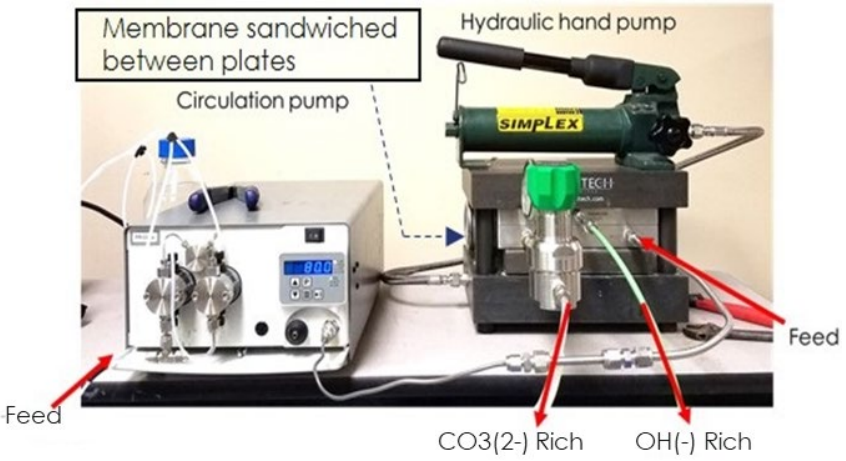

Exhibit 3.1.2. Nanofiltration setup for selectivity testing.

In addition to flux performance, from the pH [OH = $10^{-(14-pH)}$] and carbon loading measurements, the OH^- permeance, $\frac{C_{OH}^P}{C_{OH}^F}$ and carbonate permeance, $\frac{C_{CO3}^P}{C_{CO3}^F}$ were determined and are plotted in **Exhibit 3.1.4a**. C, P, and F denote concentration, permeate, and feed, respectively, and Rejection = 1-Permeance. The membrane showed excellent hydroxide permeance with almost no rejection and 25% permeance (75% rejection) of carbonate ions, where these results appear to weakly depend on the applied pressure, which may be due to a reduction of Donnan exclusion from a high concentration of counter ions (potassium) shielding the membrane negative surface charge (carboxylic group). The selectivity, defined as the hydroxide and carbonate permeance ratio, was 4, as shown in **Exhibit 3.1.4b** and conducive to enhancing carbon capture via integration with a spray absorber.

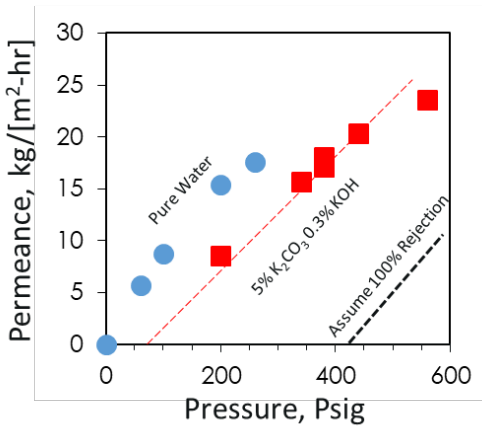

Exhibit 3.1.3. Effect of pressure on permeate flux from a feed solution containing 5 wt% K_2CO_3 and 0.3 wt% KOH using NFX membrane.

The results from membrane testing demonstrated adequate hydroxide separation and satisfied the project's requirement. Next, to demonstrate in-situ capture on the NF permeate side, the SEPA CF unit was modified as schematically shown in **Exhibit 3.1.5a** by configuring with an inlet and out port on the permeate side, and CO_2 (14% as preliminary run, 35 mL/min) was passed intermittently through one of the ports on the permeate-side to contact the permeate from the feed side via the membrane. The pH of the permeate solution was subsequently measured. During the experiment, 5 wt% K_2CO_3 was fed at 20 ml/min while a back pressure of ~80 psig was applied to the nanofiltration unit. When the gas supply to the NF membrane was turned on, gas bubbles were observed in the permeate channel. The permeate rate during CO_2 on and off was between 1-1.3 ml/min, and as shown in **Exhibit 3.1.5b**, a reduction in pH was observed when the CO_2 feed was turned on, confirming capture via KOH + CO_2 = K_2CO_3 in the NF assembly prior to the spray section of the hybrid membrane absorber. From the drop in pH, approximately 96% of the produced hydroxide was utilized.

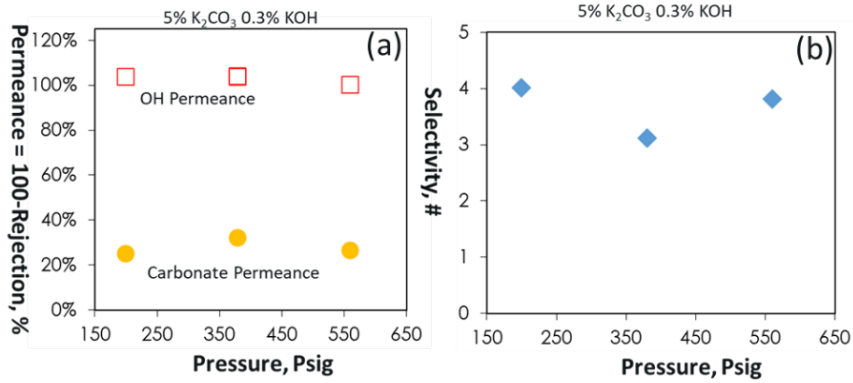

Exhibit 3.1.4. Effect of pressure on permeance (a) and selectivity (b) of hydroxide and carbonate from a solution containing 5 wt% K_2CO_3 and 0.3 wt% KOH using NFX membrane.

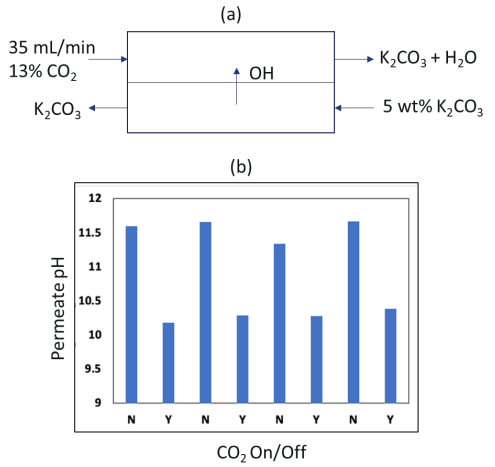

Exhibit 3.1.5. Configuration of NF unit (a) and pH of permeate during 'CO_2 on' (Y) and 'CO_2 off' (N) conditions (b).

Designation	NFX	NF270
Brand	Synder	Filmtec
Material	Polyamide	Polypiperazine
Water Permeance (LMH/bar)	~4-7.5	~17
$MgSO_4$ Rejection	99 %	99%
NaCl Rejection	40 %	50%

Exhibit 3.1.6. Comparison of Filmtec NF270 and Synder NFX membranes.

In collaboration with project partner Vanderbilt University, an additional census of membranes included Filmtec NF270. The properties of the membrane are compared to the Synder NFX in **Exhibit 3.1.6** and show similar sulfate rejection, albeit much higher permeance (>2X) for the NF270 membrane.

The NF270 membrane was tested for OH^- separation from CO_3^{2-} using a mixture of KOH and K_2CO_3 at varying concentrations of CO_3^{2-} and solution pH under a constant flux of ~30 LMH. Similar to the NFX, the results from membrane testing (**Exhibit 3.1.7**) demonstrated adequate hydroxide separation with > 75% carbonate rejection and almost no rejection of hydroxide, especially at > 1% carbonate feed. Following the promising results from the flat-sheet NF testing, a spiral wound NF270 membrane element with 7.6 m^2 was procured to continue spray absorber integration and testing. Furthermore, the results suggest that despite differences in membrane materials, polypiperazine for NF270 and polyamide for NFX, both membranes satisfied the requirement for hydroxide recovery and were consistent with the SO_4^{2-} and Cl^- rejection trend provided in **Exhibit 3.1.7** (higher selectivity for NF270 at 1 wt%), with the implication that membranes with similar specifications will be adequate for forming the membrane absorber.

NF270 CO_3 Conc. (%)	Feed/Perm	pH	CO_3 Rej (%)	OH Rej (%)	Selectivity #
0.1	Feed	11.83	83.90	39.74	3.74
0.1	Permeate	11.61			
0.1	Feed	12.96	64.45	14.89	2.39
0.1	Permeate	12.89			
1	Feed	11.84	84.54	0*	6.47
1	Permeate	11.92			
1	Feed	12.97	77.28	0*	4.40
1	Permeate	12.99			
3	Feed	11.83	78.53	0*	4.66
3	Permeate	12.29			
3	Feed	13.05	76.13	0*	4.19
3	Permeate	13.22			

Exhibit 3.1.7. Performance NF270 NF membrane for hydroxide recovery with 0.1 to 3wt% carbonate and feed pH adjustment by OH^- addition. *Negative rejections due to charge balance phenomena are normalized to zero for pessimistic calculations.

Design Membrane Absorber including NF and Spray Section for Effective DAC

To design the spray section of the hybrid membrane absorber (MA), pressure drop, flow rate, and droplet size for several spray nozzles from two vendors (BETE – PJ20, PJ24, PJ32 and Spraying Systems Co. – HP10, HP15, HP20) were considered with target flow rates and pressure below 100 LPH and 100 psig. **Exhibit 3.1.8** shows the flow rate and diameters for the BETE and Spraying Systems Co. nozzles with higher flow and droplet size (Sauter diameter) observed from the BETE spray nozzles. Based on the droplet size range, 40 to 85 µm, the estimated terminal velocities (assuming laminar flow conditions) for the water droplets range from 0.05 to 0.2 m/s, such that the superficial velocity requirement during operation is < Vt (which is proportional to the square of droplet size) to ensure a countercurrent operation and avoid significant liquid carryover scenarios. Coupled with the low flow of the Spraying Systems Co. nozzles, the BETE nozzles were procured and configured for testing in countercurrent mode with the feed air. **Exhibit 3.1.9a** shows a visualization of the spray pattern for the BETE PJ32 with a conical dispersion of the water droplets, along with the spray absorber used (**Exhibit 3.1.9b**). Three BETE nozzles, PJ20, PJ24 and PJ32, were configured and tested in the spray absorber, and their typical characteristics are listed in **Exhibit 3.1.10a**. The spray absorber has a diameter of 12 inches, and a height of 18 inches with air and solvent flow counter current during operation. Vaisala CO_2 probes installed at the air exit at the absorber top track CO_2 concentration. **Exhibit 3.1.10b** compares the performance of the three spray nozzles at 0.3 to 3.0 CFM. As shown, they had very similar performance with

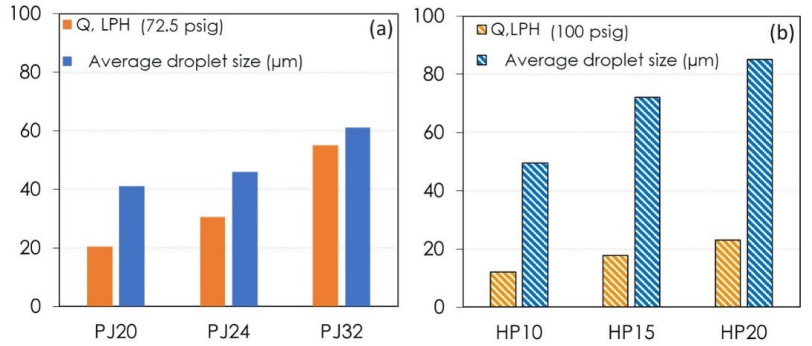

Exhibit 3.1.8. Flow and average droplet size (Sauter diameter) for spray nozzles from Spraying Systems Co. and BETE based on manufacturer specifications.

Exhibit 3.1.9. A visualization of atomized conical spray pattern with BETE PJ32 Nozzle (a) and spray absorber configuration (b).

	PJ20	PJ24	PJ32
2wt% KOH spray rate (L/min)	0.44	0.5	0.65
Nozzel pressure (psig)	120	90	40
Approximate coverage (inches)	12	16	22
Approximate spray height (inches)	6	8	11
Droplet size (µm)	41	50	62
Solution height (inches)	1.5	1.5	1.5
Air inlet above solution (inches)	3	3	3
Nozzel to solution (inches)	15.5	15.5	15.5

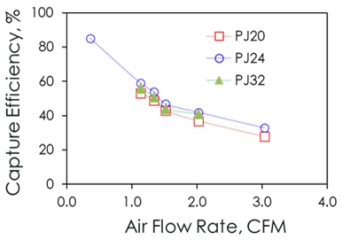

Exhibit 3.1.10. Properties of BETE nozzle (a) and capture performance during operation with 0.3 to 3 CFM Air (b).

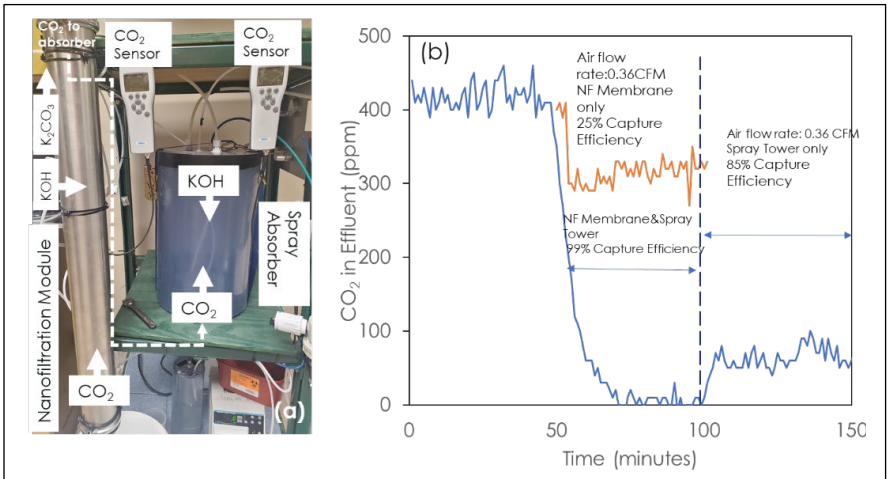

Exhibit 3.1.11. NF and spray absorber configuration (a) and performance (b) during membrane absorber operation.

a marginally higher capture efficiency performance for the PJ 24's, i.e., about 5-10% higher than the other two, with ~90% capture performance achieved at < 1 CFM. Following these results, the spray absorber equipped with the PJ24 nozzle was selected for continued testing, including coupling with NF and testing at increased residence time with a multi-nozzle configuration.

In order to couple the NF and SA for the hybrid MA, the NF membrane was serially and externally connected with the spray absorber by the airflow only, such that the air flows through the permeate channel of the NF membrane and then proceeds into the spray absorber bottom where 2wt% potassium hydroxide solution is sprayed in countercurrent mode. The NF membrane had an active area of 7.6 m^2 and was fed with 5wt% potassium carbonate at ~0.6 L/min with a resulting permeate rate of ~0.2 L/min at ~60 psig of back pressure applied, while a 2wt% at 0.5 L/min was recirculated in the spray section. An air flow rate of 0.36 CFM was used for testing. **Exhibit 3.1.11** summarizes the data for the NF membrane, spray tower and their combination. The NF membrane provided about 25% CO_2 reduction, and the spray tower achieved 85% capture efficiency. After their serial combination, the overall capture efficiency approached 99% (beyond the project requirement of 90%) with the air flow rate of 0.36 CFM, demonstrating the capture intensification capability of the integrated system.

However, the results demonstrated so far from the spray absorber generally show increased capture efficiency performance with reduced gas-side flow rate/increased residence time. Furthermore, considering droplet velocities of 0.2 m/s traversing a foot-tall absorber implies less than 1 second of contact time with air and a liquid side limit to capture performance. As such, a 55-gallon spray absorber was constructed featuring three BETE PJ24 nozzles and evaluated with and without internals promoting further gas-liquid contact as shown in **Exhibit 3.1.12**. The absorber parameters are summarized in **Exhibit 3.1.13**.

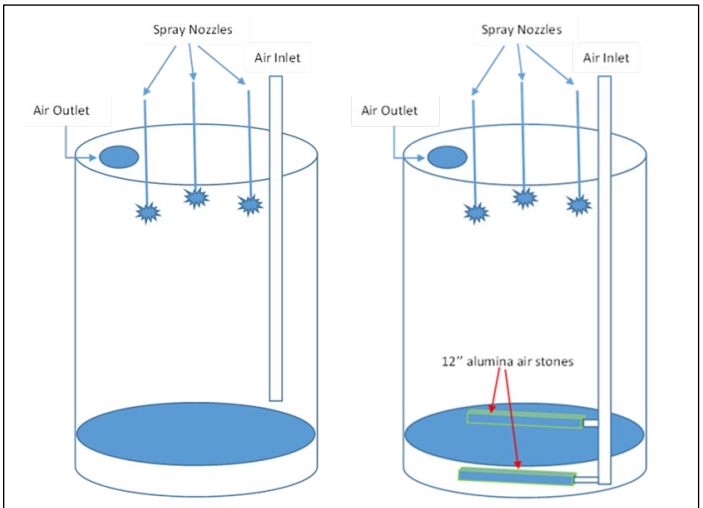

Exhibit 3.1.12. Configuration for a 55-gallon spray absorber without (left) and with (right) air stones at the air inlet.

To assess the absorber configuration, air flow rate ranging from 1.1 CFM to 4.0 CFM was tested with 2wt% KOH solution as the absorbent. The air was introduced into the drum in two ways: one with a 3/8" tube about 1 inch above the liquid and the other with two 12" air stones acting as internals attached at the end of the tube, as shown in **Exhibit 3.1.12**. Three nozzles were arranged to cover as much of the drum's cross-section area as possible, i.e., ~8 inches to the drum rim and 120 degrees apart. **Exhibit 3.1.14** describes the DAC capture efficiency using the 55-gallon drum (7.4 cubic feet empty bed volume) with and without internals. The results are compared to the integrated hybrid membrane absorber on a residence time axis. As evidenced, increasing contact via internals increased capture performance at all tested residence times. To facilitate the "internal" integration of the NF and SA units, a tubular nanofiltration membrane module (WMC110 dNF40) with a membrane surface area of 5.6 m^2 from NX Filtration Inc in the Netherlands was used. The tubular NX NF membrane was integrated with the SA to form the MA. Standalone testing of the NX membrane showed negative hydroxide rejection (-4%, i.e., unrestricted hydroxide passage). For DAC operation, the NF membrane permeate side is configured with the SA in flux enhancement mode (i.e., using make-up water as draw solvent to boost hydroxide flux) or gas pump mode (i.e., using 20-40% of influent air for permeate side fluid transport and reaction, <0.15 psig gas side pressure drop) as shown in **Exhibit 3.1.15a**. **Exhibit 3.1.15b** shows a side-by-side comparison of the performance of the SA and MA with air influent at 10 CFM and 3M KOH as the capture solvent. The NF membrane operated at ~40 psig back pressure (liquid-side). As evidenced, the MA achieved ~91% capture efficiency (and nearly 100% at maximal), satisfying the BP2 target and slightly improving the capture performance compared to the SA. Nonetheless, it is expected that by boosting gas-liquid contact time, additional gains in capture performance may be realized, even at much higher gas rates for the SA and MA. The next section describes UKy's approach to developing a high-performance ER.

The number of Nozzles	3
10 L 2wt% KOH spray rate (L/min)	1.1
Nozzle pressure (psig)	90
One Nozzle approximate coverage (inches)	16
One Nozzle approximate spray height (inches)	8
D32 at 200psi (μm)	50
Extended D32 (μm)	78
Bucket diameter (inches)	22
Bucket height (inches)	34
Solution height (inches)	2
Air inlet to solution (inches)*	1 above or 0.5 below
Nozzle to solution (inches)	30
Bucket empty bed volume (ft^3)	7.4

Exhibit 3.1.13. Experimental parameters for spray nozzle tests in the 55-gallon drum. *Note: 1 inch above the solution without airstones, 0.5 inches below the solution with airstones.

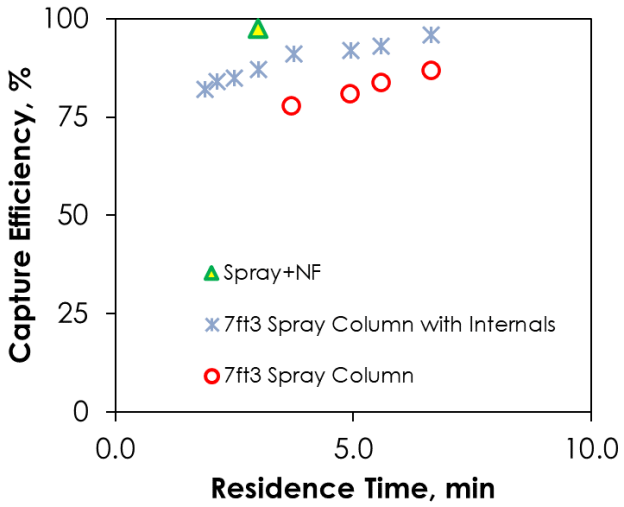

Exhibit 3.1.14. Performance of spray absorber with and without internals compared to the membrane absorber configuration.

3.2 Development of an electrochemical regenerator cell for effective DAC

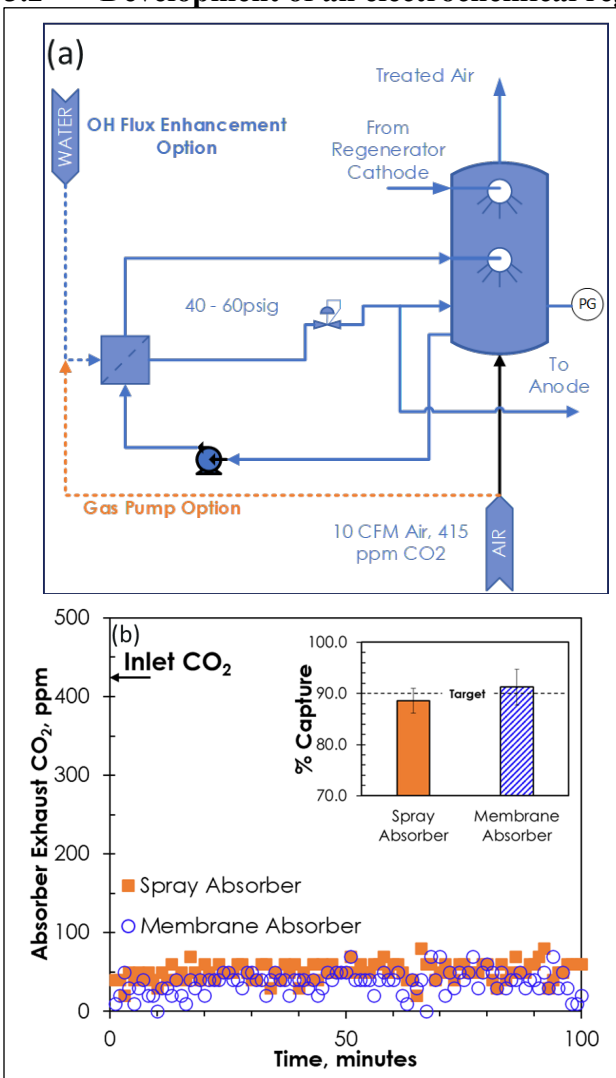

Exhibit 3.1.15. Flow diagram of membrane absorber in electrochemical DAC process (a), and performance comparison of membrane absorber and spray absorber with 10 CFM air counter-current to 3M KOH (b). Capture efficiency is shown in the inset.

Electrochemical regenerator construction

In order to develop the solvent regenerator, the initial experiment set involved electrochemical characterization in selecting electrodes that maximize current for a given voltage. Electrochemical tests were performed using a three-electrode cell configured with either Inconel (Ni-Fe-Cr), platinum (Pt), nickel (Ni), iron (Fe), nickel-iron alloy (Ni-Fe), and titanium (Ti) as the working electrode (i.e., electrode under examination, 0.36 cm^2 geometric area). The setup (**Exhibit 3.2.1**) was configured with a Hg/HgO as a reference electrode for measuring potentials and a counter graphite electrode. Cyclic voltammetry (CV, Autolab) was performed in a potassium carbonate (K_2CO_3) solution at 50 mV s^{-1} and room temperature. The CV profiles feature two regions with rapid increases in the current due to water electrolysis, one for O_2 evolution when the potential is positive and one for H_2 evolution when the potential is negative. As shown in **Exhibit 3.2.2**, different metals respond differently even at the same potential, e.g., at 1.5 V, the Inconel electrode produces >200 mA cm^{-2}; however, the current coming from the titanium electrode becomes insignificant. On the other hand, the Pt electrode offers a considerable current for H_2 production. The half-cell comparison suggests that to achieve a lower energy cost for water electrolysis, Inconel and platinum are the best candidates for positive and negative electrodes. Unlike iron, which is likely to corrode during long-term testing due to the acidified environment stemming from CO_2 release from carbonate, Inconel (Ni-Fe-Cr) is considered stable in corrosive

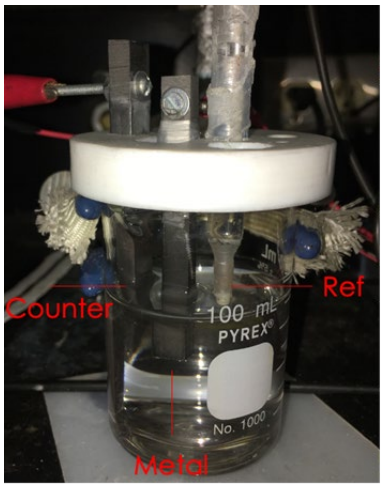

Exhibit 3.2.1. A three-electrode system to evaluate H_2 and O_2 evolutions for metal electrodes.

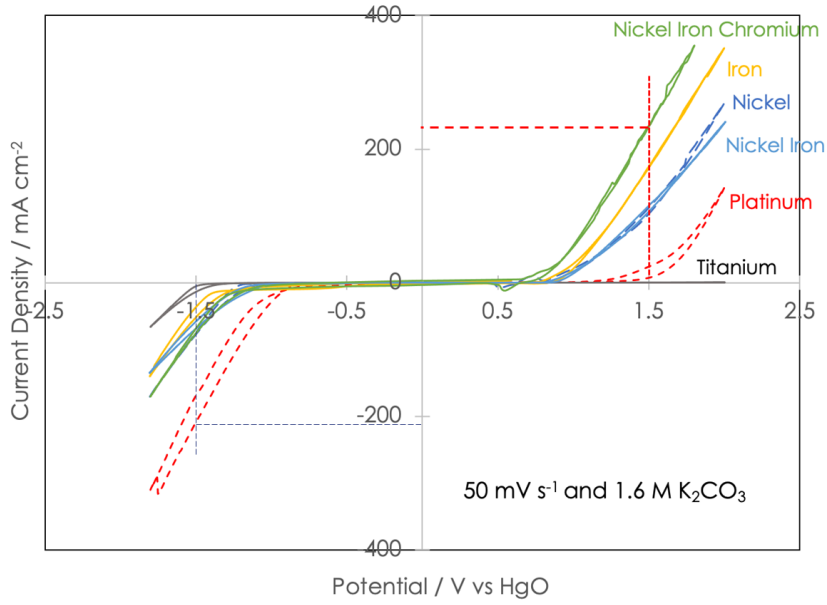

Exhibit 3.2.2. Cyclic voltammograms for Inconel (Ni-Fe-Cr), Iron (Fe), Nickel (Ni), Nickel-Iron (Ni-Fe), Platinum (Pt), and Titanium (Ti) metal electrodes in 1.6 M K_2CO_3 solution at 50 mV s^{-1} at room temperature.

environments. The Inconel (Ni-Fe-Cr) anode and a Pt-carbon cathode were selected based on the CV results for the flow cell study.

Electrochemical Regeneration Flow Cell Design

The selected Inconel and Pt-based electrodes were incorporated into flow cells as anode and cathode for flow cell testing. The electrochemical flow cell was formed with a cation exchange membrane, sandwiched by flow spaces, which are in turn sandwiched by Inconel and Pt-C as electrodes (**Exhibit 3.2.3**). A potential or current is applied to the cell via a power source. The active cell area was 16 cm^2, and the anode and cathode were spaced ~ 3 mm apart. Testing was conducted in single-pass mode with 0.27 to 0.95 M K_2CO_3 and with the test solutions fed at 5 to 15 mL/min. A constant current of 3A (~0.2 A/cm^2) was applied to the cell. During cell polarization, gas evolution can impede ion/species transport to/from the electro-reactive surface. Therefore, **Exhibit 3.2.3** supports the expectation that increased flow rate and/or salt concentration can reduce the cell voltage by improving ion conduction and quickly detaching bubbles from the electrode surface. For instance, when the flow rate of 0.55 M K_2CO_3 increases from 5 to 15 mL/min, the cell voltage decreases from 5.3 to 4.9

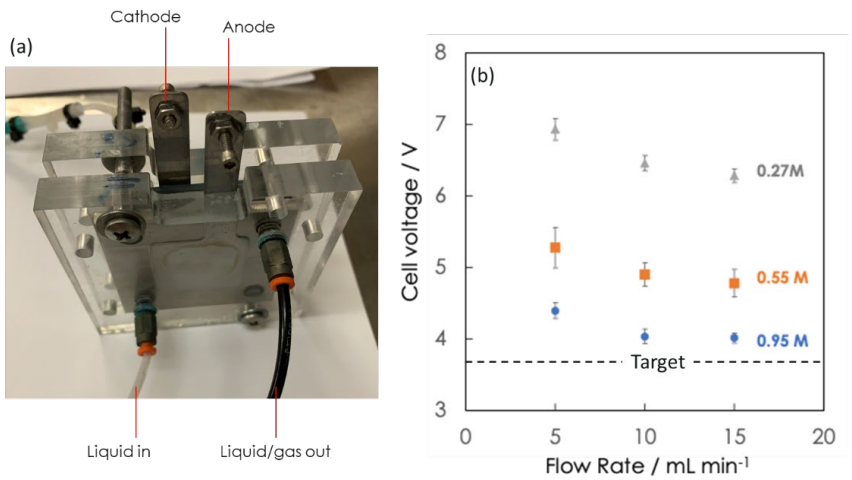

Exhibit 3.2.3. A photo of a full electrochemical flow cell (a) and a plot of cell voltage versus flow rate at 3 A under the once-through operating condition (b). The solvent regenerator was operated using 0.27 M, 0.55 M, and 0.95 M K_2CO_3 and was equipped with an Inconel anode and Pt-C cathode. The target is to limit operation below 3.7 V. A second target (not shown) is to limit operation below 2.7 V.

V. Moreover, when the K_2CO_3 concentration increases from 0.27 to 0.95 M at 10 mL/min, the cell voltage correspondingly reduces from 6.5 to 4 V. From the plot in **Exhibit 3.2.3**, it is also found that the cell voltage is more sensitive to changes in the K_2CO_3 concentration than the flow rate. For example, tripling the salt concentration reduces more than 2 V cell voltage, which is a consistent trend with **Exhibit 3.2.2,** where <3.0 V is required for 0.2 A/cm^2 with 1.6 M K_2CO_3 for an Inconel and Pt pair. For comparison, commercial electrolyzers for hydrogen production can operate at 0.5-2 A/cm^2 while requiring <3.0 V, which is facilitated by their reduced ohmic resistance (<0.5 ohm-cm^2) from zero-gap operation (the electrodes and membranes are usually tightly pressed together), higher temperature operation to improve reaction kinetics, and high-pressure operation (e.g., reducing the gas volume in solution). However, there is no concern about proton vs. potassium transport through the membrane even when cation membranes are employed since hydrogen (and oxygen) production is the only focus. In order to pursue a target of < 3.7 V at > 0.2 A/cm^2 while retaining a potassium transport efficiency of 80% or more, the cell's impedance was further reduced via zero-gap operation.

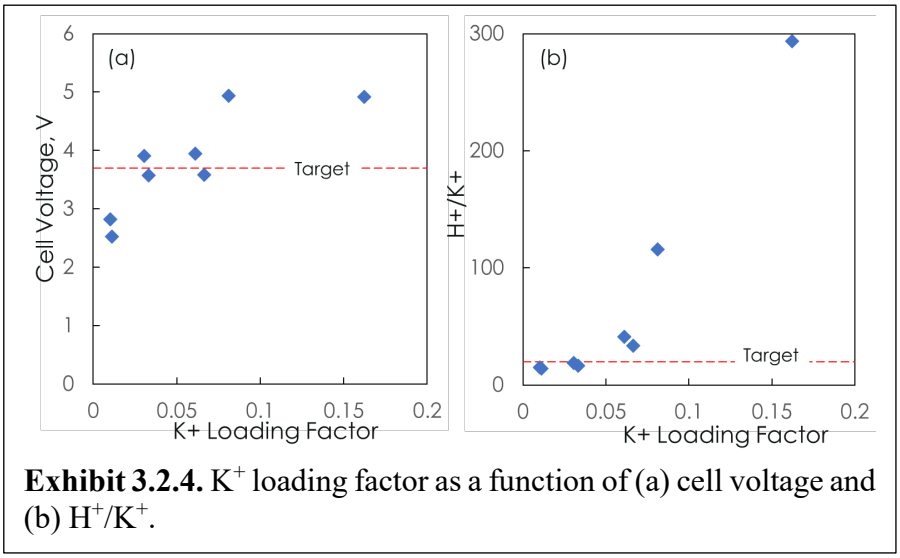

Exhibit 3.2.4. K^+ loading factor as a function of (a) cell voltage and (b) H^+/K^+.

Towards reducing voltage requirement by minimizing charge transport losses, a zero anode-cathode gap configuration was explored. In addition, the loading factor as a lumped parameter, i.e., current normalized by feed alkalinity and the flow rate, was used as a control variable since it affects pH swing and proton crossover. When the loading factor approaches unity, there is the implication that K^+ transport in low alkalinity solution can no longer support the ionic current, leading to an increased crossover of H^+ to the cathode to recombine with generated OH^- ions, reducing KOH formation efficiency for capture. All the tests were conducted at room temperature under a once-through operating mode using K_2CO_3 solutions. Test solutions samples collected from the flow cell outlet were sealed in HDPE bottles and later analyzed using alkalinity testing to determine the concentrations of K^+ and H^+. Parametric testing at 1.2-3.06 M K+ (or Alkalinity), 10-20 mL/min, and 625-1875 A/m^2 revealed that loading factors below 0.05 achieved < 20% proton crossover and <3.7 V, the interim target as shown in **Exhibit 3.2.4**. However, the internal circulation in the anodical channel with high alkalinity will prevent the H^+ from passing through the cation membrane when the ER has less than 0.05 K^+ of total alkalinity involved in ions permeation.

In order to benchmark the UKy electrolyzer against commercial electrolyzers, 3 solvent compositions, including near-saturated $KHCO_3$, 3M K_2CO_3 and 6M KOH (allowing retention of similar K concentration), were demonstrated for cell testing at room temperature and 80 °C with the results summarized in **Exhibit 3.2.5 and Exhibit 3.2.6**. As reported, when the SOA alkaline electrolyzer configured with the Ni-Fe electrodes separated by a diaphragm is tested in 6M KOH

at 75ºC, the operating voltage is about 1.94 V at 0.2 A cm^{-2}. Very similar voltage behavior is achieved for the UKy electrolyzer (**Exhibit 3.2.5c and 3.2.4**). Besides testing the conventional alkaline electrolysis, carbonate and bicarbonate electrolysis studies were also performed using the UKy electrolyzer for comparison. Compared to the hydroxide-based alkaline electrolysis, carbonate electrolysis showed diminished performance exemplified by a larger voltage requirement for the same current density, owing to the limited OH^- concentration at the anode and reduced ionic conductivity when carbonate solution is used, considering the anode reaction of $4OH^- = O_2 + 4e + 2H_2O$, and an expected higher conductance for hydroxide vs. carbonate ions, even at similar concentrations. Such conclusions can be superimposed when testing the bicarbonate solution. Moreover, increases in the temperature can reduce the cell operating voltage for bicarbonate electrolysis. Furthermore, pH measurements during carbonate electrolysis at room temperature using 0.35 M and 3M K_2CO_3 show cathode pH rise towards pH 14 to support capture in the membrane absorber. While KOH concentration had an immediate effect on polarization response and the UKy ER has been demonstrated to be on par with commercial electrolyzers, in order to reduce the energy requirements for the DAC process, anode depolarization via H_2 is expected to reduce operating voltage by > 1V to enable ER operation below 3V.

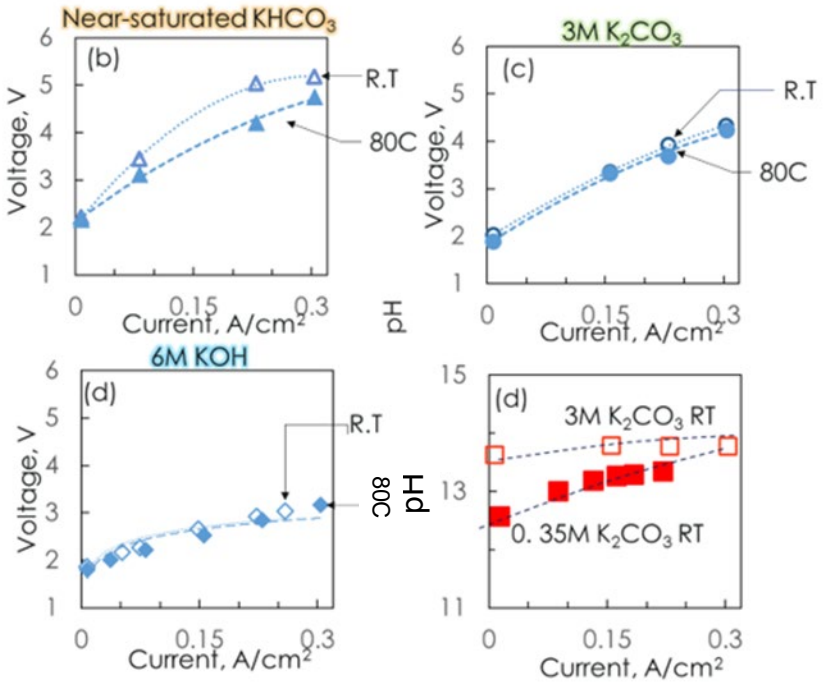

Exhibit 3.2.5. Effect of reaction kinetics on performance using near-saturated $KHCO_3$ (a), 3M K_2CO_3 (b), and 6M KOH (c). pH swing at room temperature is demonstrated with 0.35 M and 3M K_2CO_3 (d).

Case	E / V @ 0.2A cm^{-2}	Solution / M	Flowrate / mL min^{-1}	Temp. / ºC	Separator
SOA	1.94	6M KOH	N/A	75	Diaphragm
Case 1	2.06	6M KOH	150	70-80	Anionic
Case 2	2.41	6M KOH	5.5	70-80	Anionic
Case 3	2.93	6M KOH	5.5	70-80	Cationic

Exhibit 3.2.6. Case studies on the operating cell voltages.

3.3 Integration of the MA and ER for DAC

Following the set of parametric testing for the ER and MA, a larger solvent regenerator has been designed and fabricated to support integration to the MA by leveraging the experience learned from designing and testing the smaller solvent ER. The larger ER also employs Inconel as both the cathode and anode material to minimize the corrosion during the solvent reconditioning under the strong pH swing environments. A key technical challenge was the scaling up of the Inconel ER. Initial attempts to scale up the ER were abated due to enhanced wear and tear of the machining tools, which may be due to Inconel's tendency to harden when machined. Water milling was found to be successful for milling through Inconel, albeit with poor control for an embossed style structure required for a combined flow field and current collector. A sandwich structure of waterjet milled-through Inconel and a titanium base was adopted for ER fabrication. The cell features flow fields, including 25 vertical flow-through channels, with a spacing of 5 mm between each channel to support high-velocity flow to improve the mass transfer, rather than a simple open channel. A 200-um thick ion exchange membrane coupled with a 500-um thick firm gasket is embedded between the two electrodes to prevent an electrical short circuit. The membrane (or electrode) area exposed to solvent is about ~120 cm^2, approximately 8-fold larger than the ER in Task 3. The electrode-membrane assembly pairs with two Ti current collectors that are tightly compressed between two 12-mm thick polycarbonate plates to ensure solvent leakage-free testing. Pt mesh or electrodes can be employed with appropriate gaskets. The enlarged ER is shown in **Exhibit 3.3.1.,** and the cell has been leak tested at up to 1 GPM.

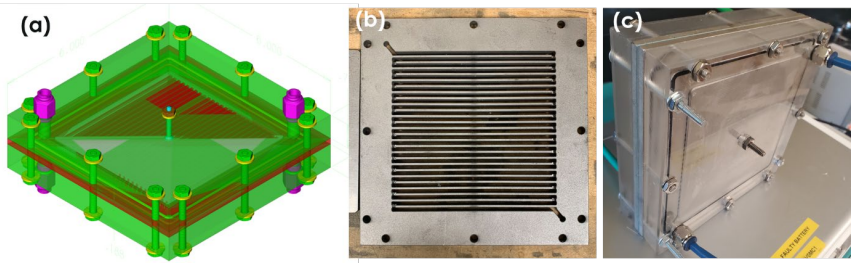

Exhibit 3.3.1. Scale-up Inconel flow ER showing (a) 3-D rendering, (b) plate-view with the serpentine flow channel, and (c) assembled cell.

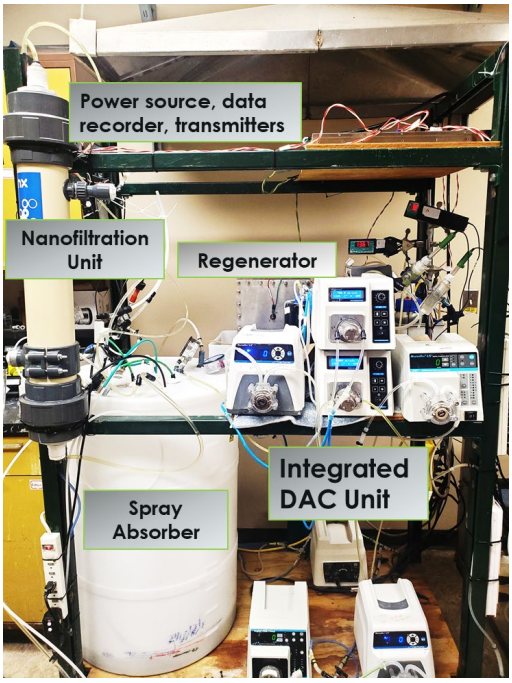

Exhibit 3.3.2. Integrated system of MA and ER.

UK IDEA integrated the membrane/spray absorber and electrochemical cell for CO_2 capture and solvent conditioning. The internal integration of the NF and SA is difficult because NF membranes are not typically scaled-up as tubular membranes, which can be tied in as a bottom section of the MA with gas pressure drop below 0.2psi. Instead, the NF membranes are scaled-up in a spiral wound architecture which amplifies the surface for liquid permeate production while gas/liquid contact is mostly restricted to only the central tube section of the module. On the other

hand, the objective to applying the NF membrane is to concentrate carbon loading (e.g., CO_3^{2-}) by removing OH^- prior to sending to the ER for regeneration with the aim of low energy consumption. Even though the in-situ NF and SA will potentially provide more surface area for CO_2 capture than the externally integrated configuration, the externally integrated NF and SA could deliver the same outcome in the view of carbon loading to ER. Currently, NF and SA integration for MA is accomplished via external connection to advance the project's requirements. **Exhibit 3.3.2** shows a picture of the integrated unit, including the MA, ER, and auxiliaries. The ER has an active surface area from 100 to 400 cm^2. The spray absorber drum volume is 55 gallons. The NF membrane is nanofiltration membrane module (WMC110 dNF40) from NX filtration Inc. A continuous approach was typically employed to facilitate testing where the solvent was conditioned by the electrochemical regenerator cell, followed by recirculation in the MA for capture.

3.4 Parametric Study and Long-term Operation

In this section, DAC operation was conducted with ~3M KOH as the starting capture solvent in the integrated membrane absorber (MA) coupled with electrochemical solvent regeneration at 10 Amperes towards achieving ≥90% carbon capture from air influent at ≥ 10 CFM for ≥100 hours. The loading factor (LF) for CO_2 recovery at the anode was controlled via a hybrid batch and continuous operation. During DAC operation, a hybrid operation was performed on the anode to boost LF to achieve lower anode pH and a larger alkalinity swing at the anode. In this mode, the ER operated in batch mode closed-loop when the pH at the ER anode exit was > 12 until the pH at the anode exit becomes ≤ 10. Then, the operation switched to continuous open-loop mode, where carbon-rich solution from the absorber enters anode recirculation and increases the pH to restart the batch mode closed-loop segment of the hybrid operation. A schematic representation is shown in **Exhibit 3.4.1.** **Exhibit 3.4.2** summarizes

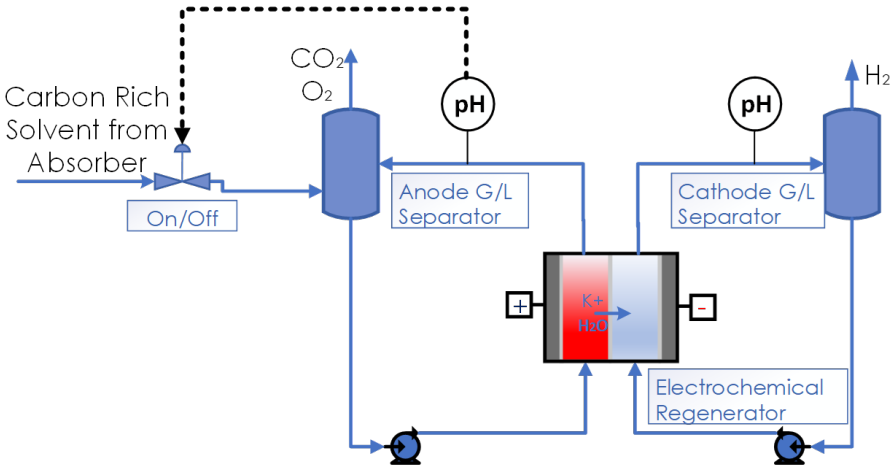

Exhibit 3.4.1. Testing scheme for the integrated DAC unit.

Nominal Loading Factor	0.4
Load factor mode	Hybrid
Starting solvent conditions	20L of 3M KOH
Air flowrate / L min^{-1}	280 (10 CFM)
Spray Absorber liquid circulation rate, L/min	1.1
NF Membrane inlet flowrate/ mL min^{-1}	800
NF Water Recovery, %	13
NF-Spray Absorber Air Split Ratio/ %	50
NF Back Pressure,psig	50
Regeneration current / A	10
Cell Temperature/ °C	70
N_2 gas for measuring CO_2 at anode / L min^{-1}	4.5

Exhibit 3.4.2. Testing conditions for the integrated DAC unit.

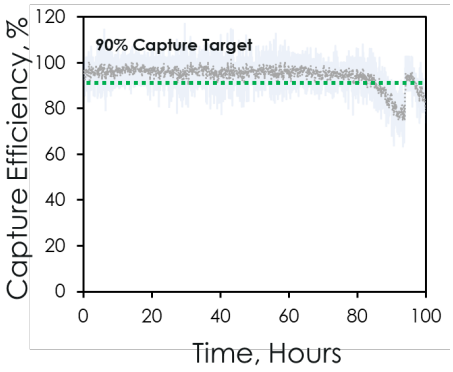

Exhibit 3.4.3. Carbon capture efficiency from 10 CFM air with ~3M potassium hydroxide solvent during DAC operation with integrated electrochemical regenerator and membrane absorber.

the test conditions during the parametric operations.

Exhibit 3.4.3 shows that carbon capture from the membrane absorber was maintained at ≥90% during the run for 100 hours duration, indicating sufficient OH^- availability (sustained by the electrochemical regenerator (ER)) for facile capture via $CO_2 + 2OH^- \rightarrow CO_3^{2-} + H_2O$. The nominal capture rate was ~107 mL /min CO_2 at 92% capture efficiency, but a maximal capture rate of ~116 mL /min CO_2 (100% capture efficiency) from 280 L/min air was also observed. **Exhibit 3.4.4.** shows the anode voltage and pH profiles during ER operation at a nominal LF of ~0.4. A minimum pH of 8.3 was initially achieved (LF > 0.4) but also corresponded to a voltage of ~3.3 V. The reduced alkalinity and OH^- concentration (pH ~8.3) is less conductive and less kinetically active, leading to higher voltage requirements. At an LF of ~0.4, a pH minimum of ~9.5 was achieved where the operating voltage was ~2.6 V and also achieved the milestone requirement of <2.7 V while facilitating OH^- production to sustain >90% capture from 280 L/min air for 100 hours (**Exhibit 3.4.3**) and carbon recovery at the anode via $HCO_3^- + H^+ = CO_2 + H_2O$ as subsequently shown in **Exhibit 3.4.5**. Furthermore, at an LF ≤ 1 for circulating anodic solution, the potassium transport efficiency is >85%.

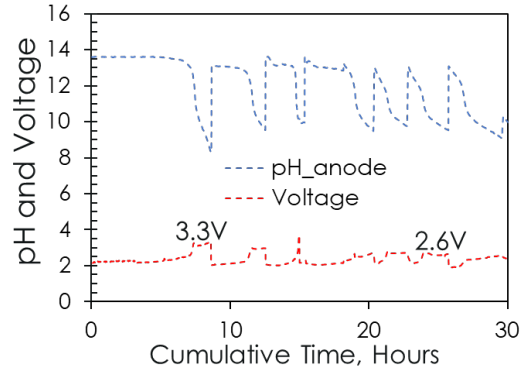

Exhibit 3.4.4. Voltage and pH profiles during DAC operation with the integrated electrochemical regenerator and membrane absorber with ~3M potassium hydroxide as the working solvent and ER operation with LF of ~0.4.

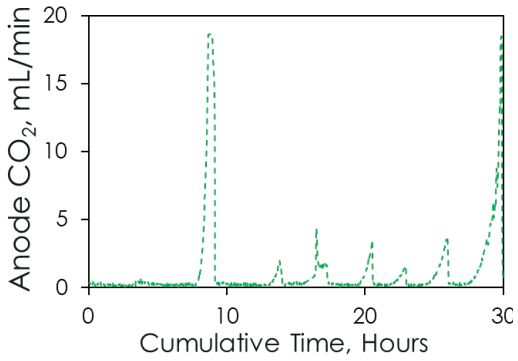

Exhibit 3.4.5. CO_2 anode exhaust profiles during DAC operation with the integrated electrochemical regenerator and membrane absorber with ~3M potassium hydroxide as working solvent.

Exhibit 3.4.5 shows that during the ER operation with LF of ~0.4 to nominally swing the pH between pH 9 to 13, CO_2 recovery was observed. A maximal CO_2 recovery rate of >17 mL/min was observed at pH 8.3 (which was limited by probe detection limit and the diluent gas), whereas it expectedly spiked to a reduced recovery of ~4 mL/min at pH 9.5. The results demonstrate enhanced desorption and recovery of CO_2 with LF toward balancing the capture and desorption rates during the operation of the DAC unit. DAC operation was subsequently

Nominal Loading Factor	~1
Load factor mode	Continuous, Flowrate modification
Starting solvent conditions	20L of 10% K_2CO_3 (~1.4M Alkalinity)
Air flowrate / L min^{-1}	280 (10 CFM)
Spray Absorber liquid circulation rate, L/min	1.1
NF Membrane inlet flowrate/ mL min^{-1}	800
NF Water Recovery, %	13
NF-Spray Absorber Air Split Ratio/ %	50
NF Back Pressure, psig	40
Regeneration current / A	10
Cell Temperature/ °C	70
N_2 gas for measuring CO_2 at anode / L min^{-1}	12.5

Exhibit 3.4.6. Testing conditions for the integrated DAC unit.

explored, including balanced carbon capture and release rates. The LF was ~1. Details of the experimental conditions are shown in **Exhibit 3.4.6.**

Exhibit 3.4.7. shows the DAC operating voltage, pH, and carbon capture and recovery rate. A nominal ER voltage of 2.7 V (10 Amps) was maintained during operation **(Exhibit 3.4.7a)**. As discussed earlier, a low pH (pH ~8.5, **Exhibit 3.4.7b**) and consequently reduced alkalinity and OH^- concentration at the anode can increase the ohmic impedance and suppresses reaction kinetics, leading to the observed higher voltage requirements. However, there is also a reduced contribution to charge leakage via $OH^- + H^+ = H_2O$ since the pH at the anode is comparatively lower compared to the ~10 to 13 swing in the prior run (**Exhibit 3.4.4**), which improves CO_2 recovery. **Exhibit 3.4.7c** shows that the nominal capture and recovery rates were balanced at ~42 mL/min CO_2 with LF ~1. The maximal CO_2 concentration from the anode exhaust is ~55% (i.e., with O_2 @ ~35 mL/min), which can be further purified downstream for transport and storage. The cost for downstream purification will be considered in the TEA. However, an ER re-design from a 2-Channel to a 3-Channel regenerator was also employed for in-situ purification.

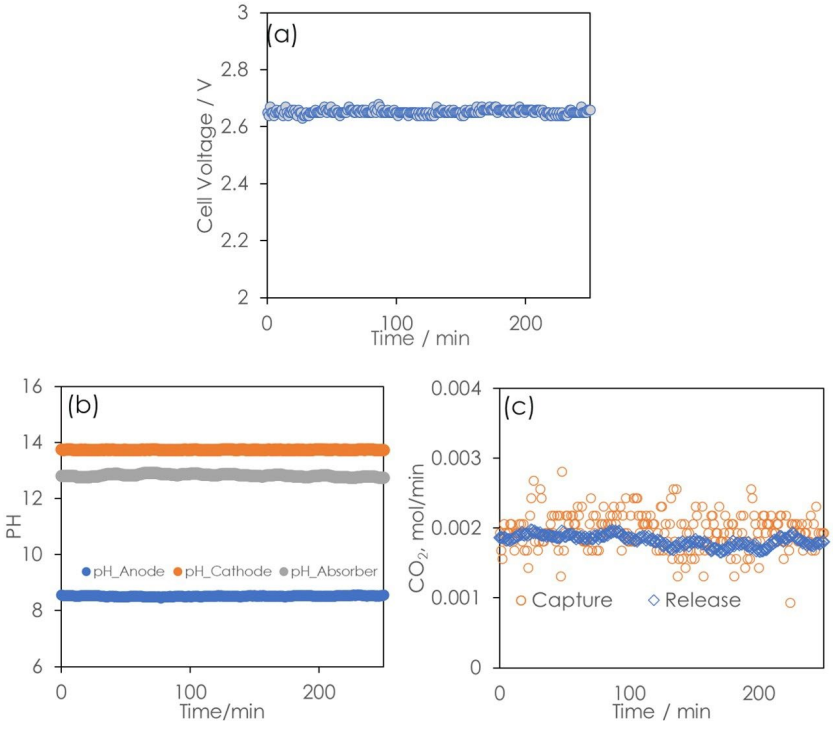

Exhibit 3.4.7. Voltage (a), pH (b), and anode CO_2 exhaust (c) profiles during DAC operation with the integrated electrochemical regenerator and membrane absorber with ~10% potassium carbonate as the working solvent and Loading Factor of ~1.

Exhibit 3.4.8a,b shows a comparative schematic of the typical 2-channel ER and an advanced 3-channel ER designed for in-situ CO_2 purification and solvent regeneration for DAC. The advanced 3-channel ER comprises the anode flow channel, an acidifying channel and

the cathode flow channel, where a bipolar membrane (BPM) separates the anode and acidifying channel. A cation exchange membrane separates the acidifying channel and the cathode channels. The BPM rectifies water into protons and hydroxide ($H_2O = H^+ + OH^-$) to supply hydroxide to the anode chamber for oxygen production (driven by electrolysis) and protons to the acidifying channel to facilitate the release of CO_2 by shifting carbonate equilibrium in the absence of O_2. In addition, potassium ions are transported through the cation exchange membrane into the cathodic channel for potassium hydroxide regeneration and hydrogen production. Although the inclusion of the bipolar membrane increases the ohmic overpotential of the ER, it allows the production of purified CO_2, which may offset the cost of downstream separation required by conventional carbonate electrolysis, especially at low CO_2 concentrations. Furthermore, the reaction kinetics at the anode can be decoupled from the carbon capture working solvent, allowing for reduced voltage losses and providing more electrode options.

Initial testing was then carried out in the cell (**Exhibit 3.4.8c**) using 0.8 M KOH fed to the anode and cathode channels and 0.9 M K_2CO_3 fed to the acidifying channel. The performance was compared to a 2-channel ER with 0.9 M K_2CO_3 + 0.2 M KOH and 6 M KOH as catholyte. The ERs were tested at the same current density of 0.05 A/cm^2, and the effect of solution resistance was compensated by deducting its impedance contribution via $E_{Compensated} = E_{measured} - iR_s$, where R_s is the solution resistance of the cell based on resistivity and cell geometry. **Exhibit 3.4.8c** confirms a best-case requirement of an additional ~0.35V for the advanced 3-channel ER vs. the 2-channel ER. However, further testing may expose additional benefits. **Exhibit 3.4.8d** confirms the pH and gas effluent results from the acidifying channel during the testing of the 3-channel ER. With increasing time, as the pH expectedly drops (BPM supplies protons to volume), CO_2 is released at the exit of this chamber with no O_2 gas detected in the effluent.

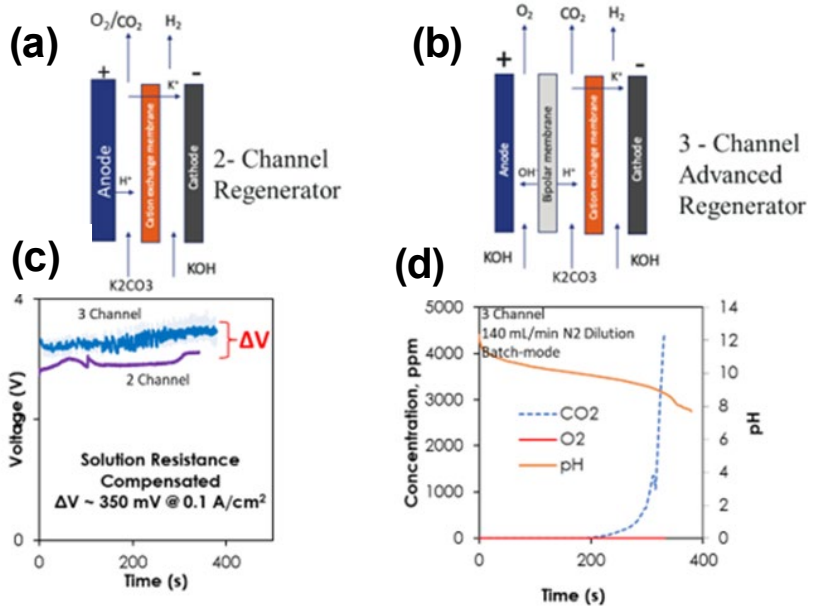

Exhibit 3.4.8. Schematic of 2-Channel ER (a) and an advanced 3-Channel ER (b) for solvent regeneration. During ER operation, (c) voltage and (d) BPM channel CO_2, O_2, and pH profiles.

3.5 Techno-economic Analysis (TEA)

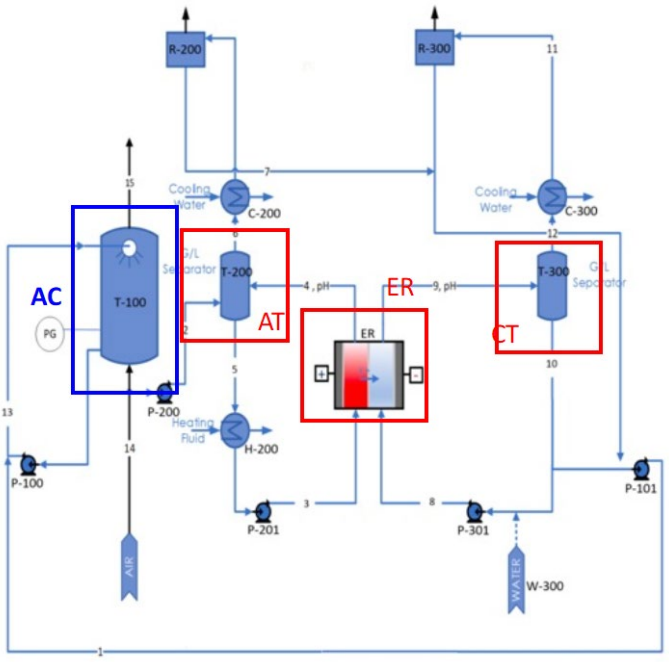

Exhibit 3.5.1. The process used to develop the TEA.

The process flow diagram depicted in **Exhibit 3.5.1** has been used to conduct TEA. In the exhibit, the delineation of the three primary components associated with the solvent regeneration process is accentuated by the red boxes. ER signifies the solvent regenerator, AT refers to the anolyte tank, and CT indicates the catholyte tank. During continuous operation, the carbon-rich solvent extracted from the absorber is directed into the anolyte tank. The anolyte pump, P-201, orchestrates the circulation of the anolyte throughout the regenerator, driving the carbonate chemistry towards the release of CO_2 gas. Concurrently, potassium ions traverse through the membrane, transitioning from the anode chamber to the cathode chamber alongside water. Notably, the process incorporates heating of the anolyte, serving dual purposes. Firstly, it diminishes the operational voltage requisite for solvent regeneration. Secondly, it expedites water transportation from the anolyte loop to the catholyte loop. This entails condensation of water in a condenser followed by its integration into the catholyte loop. Under such conditions, the meeting of K^+ ions with hydroxide ions and H_2O engenders the production of carbon-lean solvent, namely potassium hydroxide, primed for carbon capture within the CO_2 absorber.

In contrast to the intricacies of the solvent regeneration process, the carbon capture process follows a more streamlined path. The blue box highlights the CO_2 absorber, where the carbon-lean solvent descends from the apex of the absorber column, while air ingress occurs at the lower tier of the air contactor, establishing a counter-current configuration. The internal circulation pump, P-200, is tasked with optimizing OH^- utilization for carbon capture from the ambient air. Ultimately, the carbon-rich solvent is recirculated back to the solvent regeneration process.

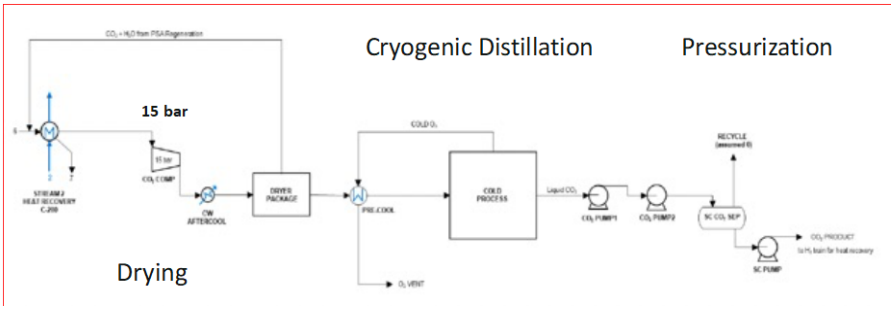

Exhibit 3.5.2. A process train used for CO_2 separation from O_2.

In TEA, CO_2 processing train is incorporated, encompassing gas drying, cryogenic distillation, and pressurization of CO_2 to meet pipeline specifications. The CO_2/O_2 stream generated at the anode side of the solvent regenerator undergoes initial cooling to condense moisture from the mixed stream. Subsequently, the cooled CO_2/O_2 mixture is compressed to 15 bar (218 psig) for cryogenic distillation. Following compression, the CO_2/O_2 stream undergoes dehydration in a pressure swing adsorption unit utilizing a molecular sieve adsorbent to eliminate water from the inlet stream. Cryogenic distillation is employed to separate CO_2, yielding a pure liquid CO_2 stream. This resulting liquid CO_2 stream undergoes dual-stage pumping to achieve supercritical pressure. The supercritical CO_2 is further pumped to pipeline utilizing a supercritical pump, elevating it to 152 bar. Subsequently, after thermal exchange with the product H_2 line, the CO_2 attains pipeline temperature standards at 30 °C (86 °F). Alongside CO_2 purification, the pure hydrogen stream generated at the cathode side of the solvent regenerator undergoes cooling, drying, and compression to align with pipeline specifications in the H_2 processing train. The dehydration unit employed for drying utilizes pressure swing adsorption technology alongside a molecular sieve adsorbent to extract water from the inlet stream. The H_2 compression system employs a four-stage compression process, incorporating intercooling after the first, second, and third stages, followed by a final aftercooler to meet the temperature specifications of the product pipeline.

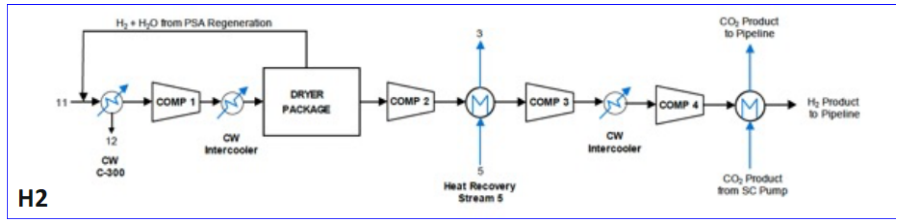

Exhibit 3.5.3. H_2 process train.

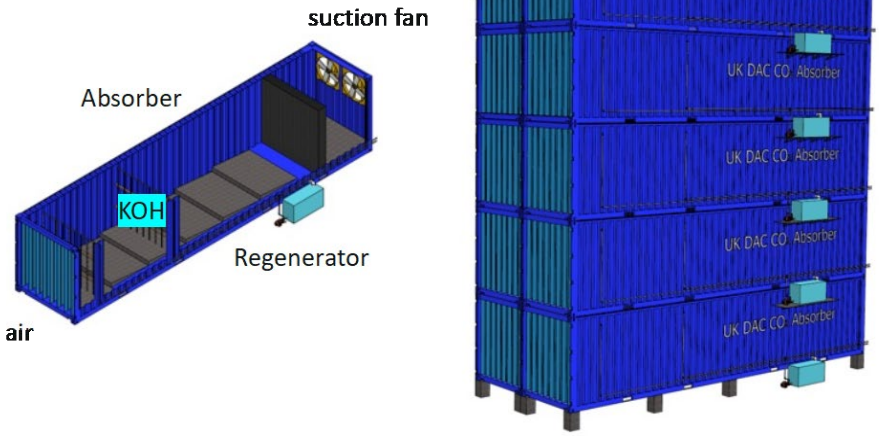

Exhibit 3.5.4. UK process scale up using a stacked shipping container.

In the TEA, a redesigned shipping container to enhance the air treatment capacity is also introduced.

As shown in **Exhibit 3.5.4**, ambient air is drawn into the DAC absorber through suction air fans positioned at the terminus of the absorber containers. Within the absorber, the air interfaces with a KOH solution in a crossflow configuration. To prevent large particulate matter from entering the system, the absorber container features an inlet air screen at the front, with air flow regulated by a simple louver system. A demister intercepts liquid droplets within the system.

Case:	611478 - UKy DAC Cogeneration of H2
Cost Base:	2022
Captured CO2, tonne/yr:	3,500
H2 Produced, tonne/yr:	235
Capacity Factor:	85%

Acct No.	Item/Description	Equip Cost	Material Cost	Labor		BEC	Eng'g CM H.O. & Fee	Contingencies		TPC
				Direct	Indirect			Process	Project	$/1000
1	Material Handling									
1.2	KOH/KHCO3 Makeup Loading to Air Contactor	1.2	0.0	0.4	0.0	1.5	0.3	0.0	0.3	2.1
	Subtotal	1.2	0.0	0.4	0.0	1.5	0.3	0.0	0.3	2.1
2	Material Preparation & Feed									
2.5	Solvent Preparation Equipment	3.3	0.1	0.7	0.0	4.2	0.8	0.0	0.7	5.7
2.6	Solvent Storage & Feed	5.6	0.0	2.1	0.0	7.7	1.5	0.0	1.4	11
	Subtotal	8.9	0.1	2.8	0.0	12	2.4	0.0	2.1	16
3	Feedwater & Miscellaneous BOP Systems									
3.4	Service Water Systems	36	3.6	18	0.0	58	12	0.0	14	83
3.7	Wastewater Treatment Equipment	20	2.0	10	0.0	33	6.5	0.0	7.8	47
	Subtotal	57	5.7	28	0.0	90	18	0.0	22	130
9	Cooling Water System									
9.1	Cooling Towers	116	0.0	35	0.0	151	30	0.0	27	208
9.2	Circulating Water Pumps	15	0.0	0.9	0.0	15	3.1	0.0	2.8	21
9.3	Circulating Water System Auxiliaries	116	0.0	15	0.0	131	26	0.0	24	181
9.4	Circulating Water Piping	0.0	32	29	0.0	61	12	0.0	11	84
9.5	Make-up Water System	4.2	0.0	5.4	0.0	10	1.9	0.0	1.7	13
9.6	Component Cooling Water System	50	0.0	38	0.0	89	18	0.0	16	122
	Subtotal	300	32	124	0.0	456	91	0.0	82	630
11	Accessory Electric Plant									
11.3	Switchgear & Motor Control	62	0.0	124	0.0	186	37	0.0	33	257
11.4	Conduit & Cable Tray	0.0	80	160	0.0	240	48	0.0	58	346
11.5	Wire & Cable	0.0	10	20	0.0	30	6.0	0.0	7.2	43
11.6	Protective Equipment	5.0	0.0	10	0.0	15	3.0	0.0	3.6	22
11.8	Misc Electrical Hardware	20	0.0	40	0.0	60	12	0.0	18	90
	Subtotal	87	90	354	0.0	531	106	0.0	120	757
12	Instrumentation & Control									
12.4	Other Major Component Control Equipment	80	0.0	160	0.0	240	48	12	90	390
12.5	Signal Processing Equipment	40	0.0	0.1	0.0	40	8.0	2.0	15	65
12.7	Programmable Logic Controllers	180	0.0	360	0.0	540	108	27	270	945
12.8	Instrument Wiring & Tubing	40	32	80	0.0	152	30	7.6	48	238
	Subtotal	340	32	600	0.0	972	194	49	423	1,638
13	Improvements to Site									
13.1	Site Preparation	0.0	7.5	160	0.0	167	33	0.0	40	241
13.2	Site Improvements	0.0	24	32	0.0	56	11	0.0	13	81
13.3	Site Facilities	23	0.0	24	0.0	48	10	0.0	11	69
13.4	Foundations	0.0	88	117	0.0	205	41	0.0	49	296
	Subtotal	23	120	333	0.0	476	95	0.0	114	686
14	Buildings & Structures									
14.4	Administration Building	0.0	10	6.5	0.0	16	3.2	0.0	2.9	22
14.7	Machine Shop	0.0	13	8.6	0.0	22	4.4	0.0	4.0	30
14.8	Warehouse	0.0	11	6.8	0.0	18	3.6	0.0	3.3	25
14.9	Other Buildings & Structures	0.0	10	7.3	0.0	17	3.5	0.0	3.1	24
	Subtotal	0.0	45	29	0.0	74	15	0.0	13	102
15	UKy DAC + H2 System									
15.1	Air Contactor System	394	39	197	0.0	630	126	315	161	1,232
15.2	Electrochemical Regenerator	w/ BEC	w/ BEC	w/ BEC	w/ BEC	2,555	511	511	536	4,113
15.3a	C-200 Cooler 1	27	37	47	0.0	110	22	11	22	165
15.3b	C-300 Cooler 2	35	46	59	0.0	140	28	14	27	209
15.3c	H-200 Heater	97	130	165	0.0	392	78	39	76	586
15.4a	P-101 Absorber Pump	43	73	99	0.0	214	43	21	42	320
15.4b	P-200 Rich Solvent Pump	12	21	29	0.0	63	13	6.3	12	93
15.4c	P-201 Anode ER Pump	13	22	30	0.0	64	13	6.4	13	96
15.4d	P-301 Cathode ER Pump	15	26	36	0.0	78	16	7.8	15	116
15.5	G/L Separators	35	3.5	17	0.0	56	11	11	12	90
15.6a	CO2 Drying and Cryogenic Distillation	w/BEC	w/BEC	w/BEC	w/BEC	2,455	491	491	516	3,953
15.6b	CO2 Pressurization	65	111	150	0.0	327	65	65	69	526
15.7	H2 Drying and Compression	w/BEC	w/BEC	w/BEC	w/BEC	535	107	0.0	96	738
15.8	RO System	w/BEC	w/BEC	w/BEC	w/BEC	62	12	0.0	11	86
	Subtotal	w/BEC	w/BEC	w/BEC	w/BEC	7,681	1,536	1,509	1,607	12,324
	Total	817	324	1,472	0.0	10,294	2,059	1,548	2,384	16,285

Exhibit 3.5.5. The total plant cost of the UK process with the capture 3.5 ktonne per year at the capcity factor of 85%.

The KOH solution reacts with CO_2 from the inlet air, yielding a potassium carbonate solution in the absorber. Subsequently, the carbonate solution undergoes processing in the ER to liberate CO_2 and regenerate the KOH solvent, concurrently generating H_2 as a co-product. Our future objective, depicted in the accompanying sketch, involves stacking 10 containers to achieve an annual CO_2 capture capacity of approximately 3,500 tonnes within the next couple of years.

Exhibit 3.5.5 presents the total plant cost (TPC) for the DAC + H2 system. These costs are calculated with a 2022 cost base year, considering a greenfield site situated in Mercer County, Kentucky. The costs are organized into subsystem account numbers following the code-of-accounts structure utilized in the DOE/NETL Solvent DAC report. Some adjustments are made to accommodate the variations between the UKy DAC + H_2 system and the DOE/NETL Solvent DAC system. Accounts 1, 2, 3, 9, 11,

Item No.	Item Name	Power Requirement, kWe
T-100	Absorber Air Fans [A]	75
ER	Electrochemical Regenerator	1,703
P-100	Absorber Recirculation Pump [B]	256
P-101	Absorber Pump	1.6
P-200	Rich Solvent Pump	0.7
P-201	Anode ER Pump	15
P-301	Cathode ER Pump	8.3
R-200a	CO_2 Drying & Cryogenic Distillation	157
R-200b	CO_2 Pressurization	2.9
R-300	H_2 Processing Train	92
RO	RO Water Treatment	5.7
WW	Wastewater Treatment Agitator	0.8
BOP	Balance of Plant	2.3
	Total Auxiliaries, MWe	**2.32**

Exhibit 3.5.6. Power consumption analysis.

12, 13, and 14 encompass balance of plant costs, site improvement expenses, and expenditures related to buildings and structures. Account 15 covers expenses specific to the UKy DAC + H_2 system, such as the air contactor/absorber system, electrochemical regenerator, heat exchangers, pumps, gas/liquid separators, CO_2 drying, cryogenic distillation, and pressurization system, as well as the H_2 drying and compression system. Additionally, the RO system for raw water treatment falls under account 15. Based upon the process flow diagram, the power consumption of the system is about 2.3 MWe for 3,500 tonne per year of CO_2 capture. Herein, **Exhibit 3.5.6** shows the power consumption breakdown.

The TEA documents the cost of CO_2 captured for the UKy-IDEA process under a 3,500 tonnes CO_2 per year (tpy) capture case and a 14X scale-up to a 49,000 tpy capture case. In both cases, the electrical consumption and energy cost are assumed to be identical, but the larger-scale case shows a significant reduction in capital cost per tonne of CO_2 captured due to the larger equipment sizing and economies of scale. Thre are four different electrical supply scenarios:

1. Current U.S. grid mix at 546 kg CO_2e/MW
2. 2050 U.S. grid mix (EIA-AEO) at 434 kg CO_2e/MWh
3. Fossil Power with CCS at 220 kg CO_2e/MWh
4. 100% Renewables at 23 kg CO_2e/MWh

The hydrogen production was credited based on three different accounting bases:

1. No GWP credit for hydrogen production in the Life-Cycle Analysis (LCA)
2. GWP credit for displacing hydrogen produced via Steam Methane Reforming (SMR)
3. GWP credit for displacing hydrogen produced via electrolysis

Overall, 12 cases were evaluated. Of the 12 scenarios, 8 were found to result in net reduction to GWP while 4 resulted in net increase in emissions. For the 8 scenarios with net abatement, a cost of CO_2 abated is calculated based on the equation below:

$$Cost\ of\ CO_2\ Abated = \text{Cost of } CO_2\ Captured \div Net\ capture\ efficiency$$

Where the net capture efficiency can be reported as the kg CO_2 abated per kg CO_2 captured in the DAC process. A perfect capture process that has no associated re-emission would have a net capture efficiency of 1, while a net capture efficiency of 0 indicates an equal amount of CO_2 is emitted elsewhere as is captured and permanently sequestered. A negative net capture efficiency indicates the operation of the plant has a net negative impact on GWP and CO_2 abatement cannot be achieved at any cost. Analyzing both the 1X and 14X scales doubles the amount of scenarios analyzed in this document from 12 scenarios to 24. **Exhibit 3.5.7.** lists the costs of CO_2 abated per tonne of CO_2 captured for each of the four electricity scenarios, each of the three hydrogen credit scenarios, and both scales analyzed in the TEA. Furthermore, there are 8 scenarios where the cost of CO_2 abated per tonne of CO_2 captured is not applicable because these cases resulted in net increase in emissions and therefore showed no CO_2 abatement.

Another contribution to the cost of CO_2 captured or abated is the sales price of the generated hydrogen from the UKy DAC + H_2 process. Hydrogen cost targets as low as \$1/kg have been proposed while current electrolysis hydrogen often fetches prices around \$10/kg. For each case, 67 kg of H_2 are produced per each tonne of CO_2 captured in the UKy DAC + H_2 process. This results in an additional credit of between \$67-670/tonne of CO_2 captured. In addition, the DAC provisions in section 45Q of the U.S. Federal tax code provide a pathway to an additional \$185/t of CO_2 captured. Together, this represents additional value streams of between \$252-855/t of CO_2 captured. These credits are not reflected in the costs of CO_2 abated presented in **Exhibit 3.5.7.**, but the impact of H_2 price on the cost of CO_2 abated is shown in the figures below.

TEA Scale	Electricity/Hydrogen Credit Scenario		
	Current U.S. Grid Mix		
	No H2 Credit	H2 SMR Credit	H2 Electrolysis Credit
1X	N/A	N/A	5,032
14X	N/A	N/A	3,090
	2050 U.S. Grid Mix		
	No H2 Credit	H2 SMR Credit	H2 Electrolysis Credit
1X	N/A	N/A	3,443
14X	N/A	N/A	2,115
	Fossil Power with CCS		
	No H2 Credit	H2 SMR Credit	H2 Electrolysis Credit
1X	1,366	1,811	1,600
14X	839	1,112	983
	Renewables		
	No H2 Credit	H2 SMR Credit	H2 Electrolysis Credit
1X	1,340	818	1,188
14X	823	502	730

**units are \$ per tonne CO2 captured*

Exhibit 3.5.7. Costs of CO_2 Abated in Different Electricity, Hydrogen Credit, and TEA Scale Scenarios*

Cost of CO_2 Abated Without Using GWP Credit from Displacing H_2

Exhibit 3.5.8. shows the cost of CO_2 abated when no credit from displacing H_2 is applied. Here, the 1X and 14X scales for the scenarios that use electricity from fossil power with CCS and from renewables are considered. The electrical supply scenarios using the current U.S. grid mix and the expected 2050 U.S. grid mix did not show CO_2 abatement and are not included on this graph. The scenarios where the UKy DAC + H_2 process at the 14X scale does not use credit from displacing H_2 show costs of CO_2 abatement less than the current value of the 45Q carbon credit for both viable electricity scenarios. At the 14X

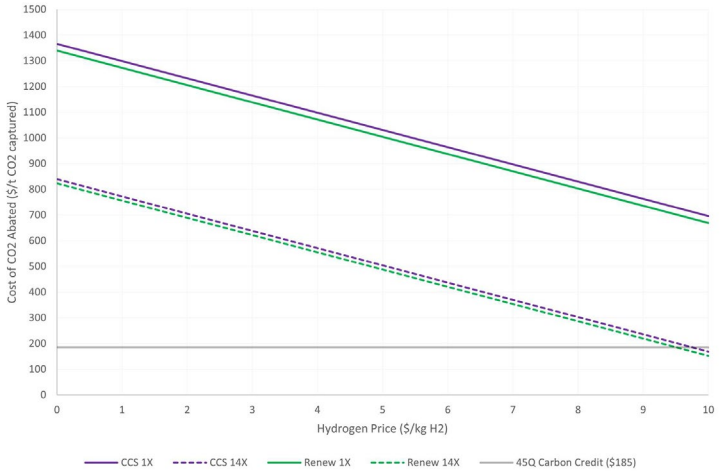

Exhibit 3.5.8. Cost of CO_2 Abated Without Using Credit from Displacing H_2.

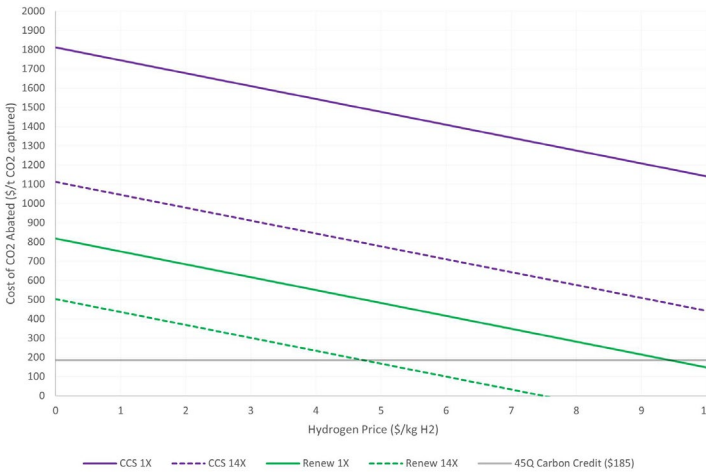

Exhibit 3.5.9. Cost of CO_2 Abated Using Credit from Displacing H_2 from SMR

scale, a hydrogen price of at least \$10/kg H_2 would be needed to achieve price parity with 45Q carbon credits.

Cost of CO_2 Abated Using GWP Credit from Displacing H_2 from SMR

Exhibit 3.5.9. shows the cost of CO_2 abated when credit from displacing H_2 produced from SMR is applied. Here, the 1X and 14X scales for the scenarios that use electricity from fossil power with CCS and from renewables are considered. The electrical supply scenarios using the current U.S. grid mix and the expected 2050 U.S. grid mix did not show CO_2 abatement and are not included on this graph. The scenarios where the UKy DAC + H_2 process at the 1X and 14X scales uses renewable electricity show costs of CO_2 abatement less than the current value of the 45Q carbon credit. For the renewable electrical supply scenario at the 1X scale, a hydrogen price of around \$10/kg H_2 would be needed to achieve price parity with 45Q carbon credits. This would be reduced to around \$5/kg H_2 at the 14X scale. For the fossil power with CCS electrical supply scenario at the 14X scale, a hydrogen price of around \$14/kg H_2 would be needed to achieve price parity with 45Q carbon credits.

Cost of CO_2 Abated Using GWP Credit from Displacing H_2 from Electrolysis

Exhibit 3.5.10. shows the cost of CO_2 abated when credit from displacing H_2 produced from electrolysis is applied. Here, the 1X and 14X scales for each of the four electricity scenarios are considered. The scenario where the UKy DAC + H_2 process at the 14X scale uses renewable electricity shows a cost of CO_2 abatement less than the current value of the 45Q carbon credit. For the renewable electrical supply scenario at the 1X scale, a hydrogen price of around \$15/kg H_2 would be needed to achieve price parity with 45Q carbon credits. This would be reduced to around \$8/kg H_2 at the 14X scale. For the fossil power with CCS electrical supply scenario at the 14X

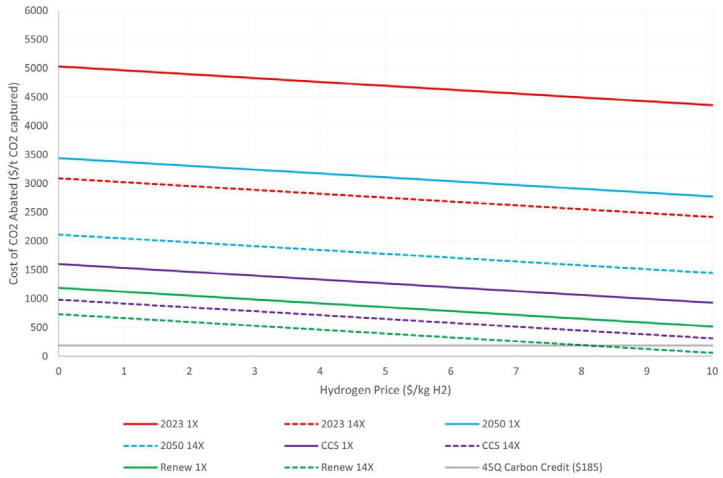

Exhibit 3.5.10. Cost of CO_2 Abated Using Credit from Displacing H_2 from Electrolysis

scale, a hydrogen price of around \$12/kg H_2 would be needed to achieve price parity with 45Q carbon credits. The higher carbon intensity electricity grid mix scenarios are unlikely to be economic with revenue solely from hydrogen sales and 45Q carbon credits. The most optimistic of these scenarios show a hydrogen price of around \$30/kg H_2 required for cost parity with the 45Q carbon credits.

3.6 Life-cycle Analysis (LCA)

An LCA was performed to demonstrate the potential of the proposed electrochemical aqueous process to be a substantive DAC option. The LCA was conducted in accordance with SOPO Appendix D. A primary concern for commercial-scale operations would involve effective hydrogen production and storage management. The design for the regenerator should emphasize the isolation of hydrogen from oxygen and potential ignition sources, good ventilation and installation of appropriate monitoring and warning systems with automated shut-down protocols. National and international standards have been established and can be used to address these recommendations (e.g., NFPA 2 and other NFPA standards, ANSI/AIAA G-095A-2017 and ISO/TR 15916). The direct air capture technology assessed in this LCA is at TRL 3, signifying that it is currently under development at bench scale. The purpose of performing a LCA for technology at this scale is to assess the performance and applicability of the DAC process.

An LCA of an electrochemical direct air capture system that cogenerates hydrogen was conducted to compare its environmental impacts to those of a system that produces the same products. This study utilizes the Tool for Reduction and Assessment of Chemicals and Other Environmental Impacts (TRACI) 2.1 method combined with the latest global warming potential (GWP) factors included in the Intergovernmental Panel on Climate Change (IPCC) Fifth Assessment Report (AR5) report. The following impact category has been modeled and is included in this report: global warming potential (kg CO_2e), based on IPCC AR5, 100-year time horizon, accounting for carbon climate feedback. The LCA for this project was conducted using openLCA including 1) Modified NETL CO2U openLCA LCI Database with project LCA, 2) Completed results interpretation spreadsheets from the PIs and 3) Completed NETL CO2U LCA Report Template. The specific goals of this LCA are described below:

1. Intended application – The intended application of this LCA is to compare the life cycle greenhouse gas (GHG) impact of the proposed project – an electrochemically-driven solvent-based direct air capture system that cogenerates hydrogen, as modeled of a *Proposed Product System*, to a *Comparison Product System*.
2. Reasons for carrying out the study – To understand how the environmental impact (measured as life cycle GHG impact) of the "Electrochemically Regenerated Solvent for Direct Air Capture with Cogeneration of Hydrogen at Bench-Scale" life cycle compares to the life cycle of a system that produces the same products.
3. Intended audience – The intended audience for the LCA described herein is the United States (U.S.) Department of Energy (DOE) Carbon Utilization Program and all stakeholders looking to evaluate, develop, or pursue DAC.
4. Public disclosure – This LCA conducted as part of the U.S. DOE Funding Opportunity Announcement (FOA) requirement will become part of the public record for the award within the final scientific/technical report.

The experimental results from the lab scale component and full system testing were used to create the most representative full-scale flow sheets and heat and material balances for the absorption and regeneration sections of the process. Existing equipment was assumed to be used for the CO_2 and H_2 purification and compression. The overall energy consumption, consumables are reported in the accompanying TEA. Material flows and inventories from this TEA were used as the inputs to this LCA.

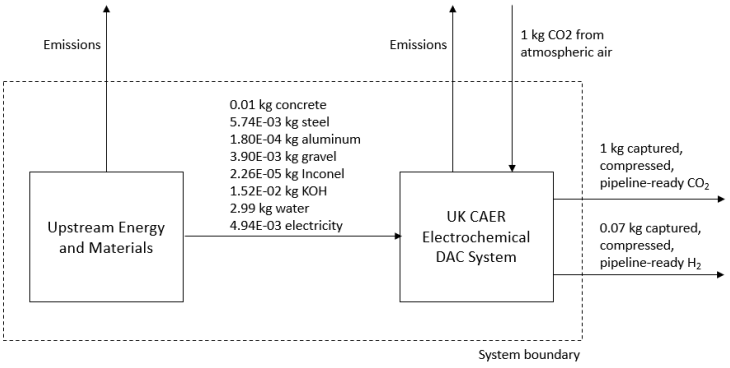

Exhibit 3.6.1. LCA System Boundary for UK Electrochemical DAC Process

The LCA was performed based on the capture and permanent sequestration of 1 kg of CO_2 from the atmosphere, and the associated coproduction of hydrogen. The hydrogen coproduction is assessed with three different accounting methods: 1) not accounting for any benefit from the coproduct; 2) accounting for hydrogen as offsetting hydrogen production from SMR; and 3) accounting for the produced hydrogen as offsetting hydrogen production from electrolysis.
For each of these accounting cases, the overall impact was assessed at the four different carbon intensities corresponding to:

1. The current U.S. grid mix: 546 kg CO_2e/MWh
2. 2050 U.S. grid mix (EIA-AEO): 434 kg CO_2e/MWh
3. Fossil Power with CCS: 220 kg CO_2e/MWh
4. 100% Renewables: 23 kg CO_2e/MWh

The life cycle stages included in the study are:

1. Materials extraction for all construction and chemical inputs to build and operate the electrochemical DAC system.

2. Operating the electrochemical DAC system to produce carbon dioxide and cogenerate hydrogen (excluding emissions during construction, commissioning, and end of life). This stage includes:

a. Starting and operating the electrochemical DAC system, a technology that includes an absorber, two gas-liquid separators, electrochemical regenerator, CO_2 processing train, H_2 processing train, and balance of plant equipment.

b. Generating CO_2 at pipeline specifications and H_2 at pipeline specifications.

For the purpose of this study, CO_2 transport and storage is an identical life cycle stage for the electrochemical DAC system and the steam methane reforming system. Furthermore, this is considered to be a cradle-to-gate study because it excludes analysis of transport and storage of the final product. Emissions during upstream process construction, commissioning of the DAC system, and end-of-life process teardown are also excluded from this study. **Exhibit 3.6.1.** represents the system boundary of this LCA, which depicts one life cycle stage for material and energy inputs and one for the electrochemical DAC system that produces carbon dioxide and hydrogen.

The Proposed Product System is a 3,500 ton of CO_2 per year capture facility. While this is a smaller than envisioned full-scale plant that could be expected to be 100 times larger, it is a significant scale up from the current process which has been experimentally developed at lab scale by UKy. This electrochemical DAC system is currently a proof-of-concept technology with multiple components that have been identified and proven at laboratory scale, which qualifies it as TRL 3. For the electrochemical DAC system assessed in this project, a screening-level LCA has been performed. This analysis allows for approximations and assumptions for the process of study in order to provide an initial estimate of the life cycle GHG emissions. While a full-scale system will have significant reduction in capital cost per ton of CO_2 captured due to the economies of scale in large installations, the electrical consumption, which makes up the vast majority of the LCA impact for all categories, is expected to remain near constant with increased size. Because of this, the LCA at the small scale is expected to be highly representative of the LCA at larger or commercial scales and no additional adjustments are required at this level of analysis. Commercial performance expectations for the electrochemical DAC system assessed in this project consist of achieving the performance shown at the lab scale in a steady state, real environment with variable ambient conditions. Electrochemical regenerator performance is expected to see slight improvement with optimized cell geometry and balance of plant operation, including CO_2/O_2 purification is expected to perform similar to existing cryogenic separation units in operation. Hydrogen and CO_2 products are expected to be produced at pipeline ready conditions, but offtake or use of each has not been assessed for this study or the envisioned commercial applications. Further scale up testing, component development and optimization including absorber, electrochemical regenerator (membrane, electrode, and geometry), and purification steps as well as the overall system operation will need to be proven and tested to assess the impact more accurately at commercial scale. With this technology being at TRL 3, the default scenario for evaluating market effects is one carbon utilization production facility. In this scenario, there is minimal to no market consequence for elastic markets. Electricity is not a product of the electrochemical DAC system in this project, so analysis of electricity production with elastic market effects is not required. Hydrogen production is expected to grow faster than supply in all regions as sectors transition to lower carbon energy carriers. Two Comparison Product Systems for hydrogen are evaluated for this project: Steam Methane Reforming (SMR) and Hydrogen Electrolysis. While most hydrogen is currently produced by SMR, the associated carbon emissions have driven research into using hydrogen produced via electrolysis as a lower carbon alternative. SMR for this study is taken to be a standalone process as described by the industry standard 'Hydrogen Production – Steam Methane Reforming – US' as modeled in the openLCA CO_2U database. Electrolysis is taken to be a standalone process using the same carbon intensity of electricity as is used for the DAC process and consuming 50 kWh/kg CO_2. This energy consumption is lower than current 'best in class' electrolysis installations but likely to be industry standard in the target installation year of 2025. These values are taken to be representative of the different methods of standalone hydrogen generation and are the basis for comparison with the electrochemical DAC process with cogeneration of hydrogen assessed in this LCA.

This subsection presents the results of the LCA when assessed with four electricity carbon intensity cases and three hydrogen product cases. Specifically, each electricity case is highlighted with visual data representing the impact of the electrochemical DAC system in terms of kg CO_2e on global warming potential.

Current U.S. Grid Mix

The GHG emissions for the proposed DAC + H_2 system is assessed at the current U.S. Grid carbon intensity of 546 kg CO_2e/MWh. Results are shown in **Exhibit 3.6.2.** This shows an overall net impact of an increase of 1.39 kg CO_2 emitted per kg of CO_2 captured and permanently sequestered if no credit for the hydrogen generation is taken, an increase of 0.86 kg CO_2 emitted per kg of CO_2 for the case where the H_2 production displaces SMR, and 0.22 kg CO_2 abated for the case where the H_2 production displaces H_2 produced via electrolysis.

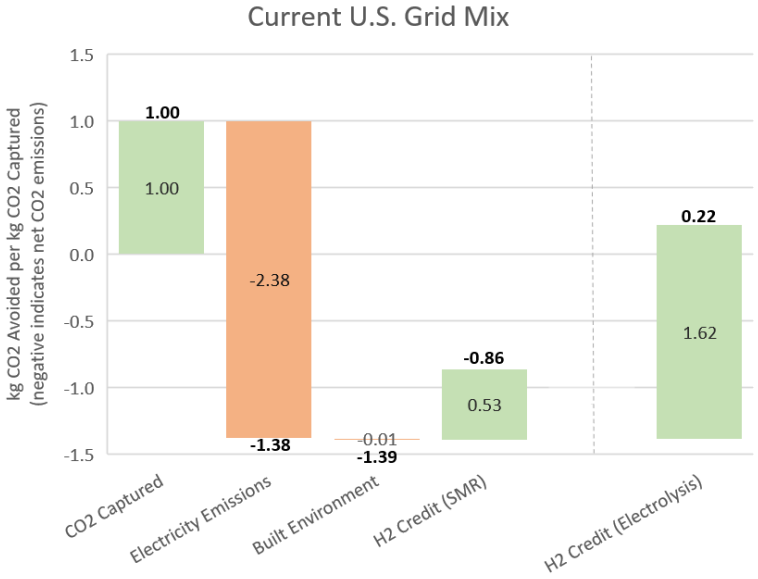

Exhibit 3.6.2. Amount of CO_2 Avoided per kg CO_2 Captured with Current U.S. Grid Mix

2050 U.S. Grid Mix

The GHG emissions for the proposed DAC + H_2 system is assessed at the expected 2050 U.S. Grid carbon intensity of 434 kg CO_2e/MWh. Results are shown in **Exhibit 3.6.3.** This shows an overall net impact of an increase of 1.08 kg CO_2 emitted per kg of CO_2 captured and permanently sequestered if no credit for the hydrogen generation is taken, an increase of 0.55 kg CO_2 emitted per kg of CO_2 for the case where the H_2 production displaces SMR, and 0.32 kg CO_2 abated for the case where the H_2 production displaces H_2 produced via electrolysis.

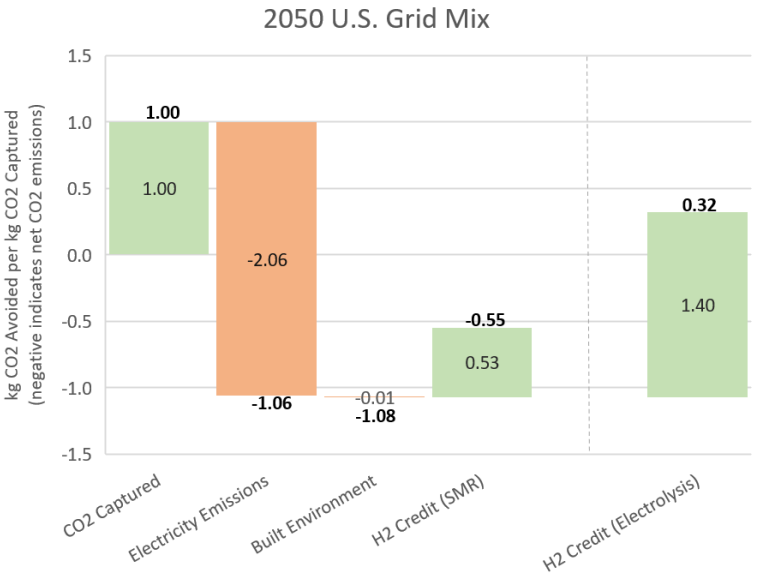

Exhibit 3.6.3. Amount of CO_2 Avoided per kg CO_2 Captured with 2050 U.S. Grid Mix

Fossil Power with CCS

The GHG emissions for the proposed DAC + H_2 system is assessed assuming that the carbon intensity of electricity is consistent with fossil generation and carbon capture and storage: 220 kg CO_2e/MWh. Results are shown in **Exhibit 3.6.4.** This shows an overall net impact of 0.08 kg CO_2 abated per kg of CO_2 captured and permanently sequestered if no credit for the hydrogen generation is taken, 0.61 kg

CO_2 abated per kg of CO_2 for the case where the H_2 production displaces SMR, and 0.70 kg CO_2 abated for the case where the H_2 production displaces H_2 produced via electrolysis.

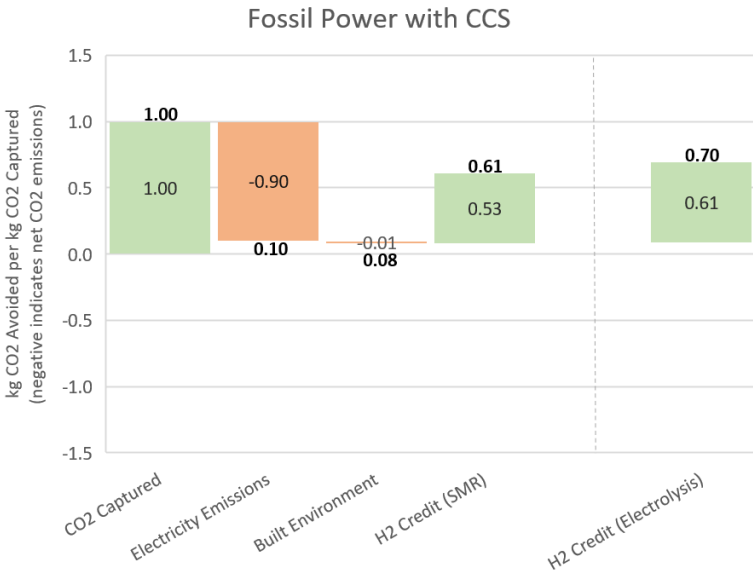

Exhibit 3.6.4. Amount of CO_2 Avoided per kg CO_2 Captured with Fossil Power with CCS.

Renewables

The GHG emissions for the proposed DAC + H_2 system is assessed with electricity generation consistent with renewable generation with a carbon intensity of 23 kg CO_2e/MWh. Results are shown in **Exhibit 3.6.5.** This shows an overall net abatement of 0.83 kg CO_2 emitted per kg of CO_2 captured and permanently sequestered if no credit for the hydrogen generation is taken, abatement of 1.36 kg CO_2 emitted per kg of CO_2 for the case where the H_2 production displaces SMR, and 0.94 kg CO_2 abated for the case where the H_2 production displaces H_2 produced via electrolysis.

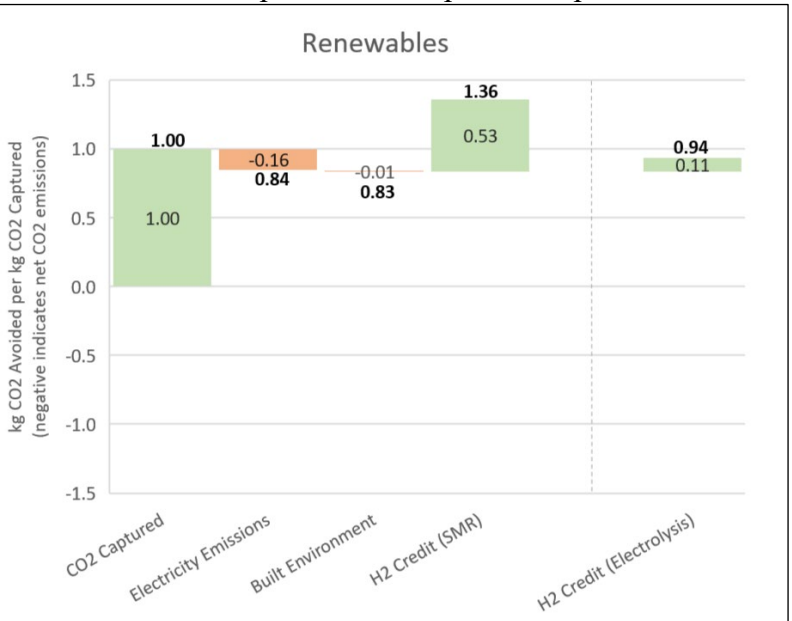

Exhibit 3.6.5. Amount of CO_2 Avoided per kg CO_2 Captured with Renewables

The results were summarized in **Table 3.6.6**. In this table, negative values indicate overall net reduction in atmospheric CO_2 concentration while positive values indicate net increase in atmospheric CO_2. It demonstrates that the overall process impact can be either positive or negative depending on the scenarios and hydrogen accounting method. This indicates that a project-specific and location-specific analysis would be required to determine the true impact of a specific installation. Process improvements such as decreasing the voltage or current required for the system will not be sufficient to achieve a net abatement in the current U.S. grid mix with no H_2 credit scenario, while almost any variation of this process would yield a significant abatement when

utilizing low-carbon renewable electricity. The uncertainty in the carbon intensity of the expected deployment scenario far outweighs any uncertainty in the process or built environment modeling.

Electricity Scenario	Hydrogen Credit Scenario		
	DAC with No H2 Credit	DAC with H2 SMR Credit	DAC with H2 Electrolysis Credit
Current U.S. Grid Mix	1.394	0.862	-0.220
2050 U.S. Grid Mix	1.078	0.546	-0.321
Fossil Power with CCS	-0.081	-0.614	-0.695
Renewables	-0.830	-1.362	-0.935

Exhibit 3.6.6. kg CO_2e GWP impact per kg CO_2 captured

4. CONCLUSION

UK IDEA DAC system comprises an ER and MA working synergistically to (1) directly remove CO_2 from air; (2) produce H_2 for sale, energy storage, grid-management, and depolarization to directly reduce the energy requirement for DAC; and (3) avoid high-temperature requirement while simplifying water management and integration with renewable energy storage like solar cells. The project results verified that UK IDEA integrated approach addressed the complexities of incumbent DAC systems by demonstrating at ambient conditions, including (1) low gas-side pressure-drop facile CO_2 capture via a membrane/spray absorber with in-situ generated hydroxide as capture solvent, (2) multi-functional electrochemical regenerator for hydroxide regeneration, CO_2 concentration and ultra-pure H_2 production after dehumidification, and (3) the TEA indicates the potential to achieve a cost of approximately $680 per tonne of CO_2 captured. Furthermore, the LCA highlights the potential for CO_2 reduction, taking into account the advantages of hydrogen production and the adoption of renewable energy.

5. AREAS OF FUTURE INTEREST

UK IDEA developed a simple two-unit operation yet effective DAC technology through this project. In order to advance this methodology, the following areas have been identified as "important" for the next step: 1. Exploring ER toward achieving $100/ton target by enhancing the catalytic functions of the electrodes. 2. Performance of the integrated system at a pilot-scale at > 40 ton/year toward the cost reduction due to economies of scale.

6. LIST OF EXHIBITS

7. ACKNOWLEDGEMENTS

The completion of this project leveraged organizational participation by UK IDEA, EPRI, Vanderbilt University, and PPL.

8. LIST OF ABBREVIATIONS AND ACRONYMS

DOE – Department of Energy
DAC – Direct air capture
ER – Electrochemical regenerator cell
MA – Membrane/spray absorber
PI – Principal investigator
TRL – Technology Readiness Level
TMP – Technology Maturation Plan
TEA – Techno-economic Analysis
LCA – Life-cycle Analysis
UK IDEA – University of Kentucky Institute for Decarbonzation and Energy Advancement